

Evolving Robustness–Exploration Trade-off in Online Reinforcement Learning via Quantile Bayesian Risk MDPs

Meichen Song

*School of Industrial and Systems Engineering
Georgia Institute of Technology
Atlanta, GA 30332, USA*

msong97@gatech.edu

Yuhao Wang

*School of Industrial and Systems Engineering
Georgia Institute of Technology
Atlanta, GA 30332, USA*

yuhaowang@gatech.edu

Enlu Zhou

*School of Industrial and Systems Engineering
Georgia Institute of Technology
Atlanta, GA 30332, USA*

enlu.zhou@isye.gatech.edu

Abstract

In online reinforcement learning, data scarcity creates epistemic uncertainty that makes robustness important early in learning, whereas sufficient exploration is needed to learn the true-environment optimal policy. We study this time-varying robustness–exploration trade-off through a quantile Bayesian risk-aware Markov decision process (BR-MDP), in which the quantile level controls how posterior uncertainty enters the Bellman backup. We characterize this control through an asymptotic normality result for the difference between the quantile BR-MDP value and the value in the true environment. The result implies that upper/lower-tail quantiles induce optimism/pessimism towards epistemic uncertainty, and the magnitude of the optimism/pessimism decreases as data accumulate. Building on this characterization, we propose an online Bayesian risk-aware algorithm with an adaptive quantile schedule that emphasizes robustness early and gradually encourages exploration of less-visited state–action pairs. We establish sublinear Bayesian regret bounds with respect to both the true optimal value and the optimal BR-MDP robust value. Numerical experiments demonstrate strong performance in both exploration-demanding and exploration-costly environments.

Keywords: online reinforcement learning; Bayesian risk optimization; Markov decision process

1 Introduction

In online reinforcement learning (RL), an agent sequentially interacts with an unknown environment and uses collected data to estimate the unknown environment and update the policy used in subsequent interactions. Thus, each action affects both the immediate reward and the information available for future decisions. Limited data lead to epistemic uncertainty in estimating environment parameters (Der Kiureghian and Ditlevsen 2009). This uncertainty is central to the consideration of exploration–exploitation trade-off (Jaksch

et al. 2010, Osband et al. 2013, Azar et al. 2017, Ma and Lee 2026): exploitation chooses actions that appear optimal under current estimates to pursue high estimated cumulative reward, whereas exploration collects information to reduce epistemic uncertainty.

Although regions with higher uncertainty offer a greater incentive to explore, acting in such regions is also risky because the unreliable estimates induce estimated optimal policies that can perform poorly in the true environment. This risk is most pronounced early in learning, when data are scarce. It is particularly salient in high-stakes settings with limited interaction budgets (Dulac-Arnold et al. 2021), such as public health intervention problems (Liang et al. 2025) and inventory or service systems with costly trial-and-error decisions. Therefore, beyond the classical exploration–exploitation consideration, the robustness of the policy used in interactions (which we refer to as the interaction policy throughout the rest of the paper) is also a primary concern early in learning, as it hedges against the risk induced by acting under epistemic uncertainty. As learning progresses and more data are collected, epistemic uncertainty decreases and such unreliable estimates become less likely. Consequently, the need for robustness becomes less essential, whereas exploring less-visited state-action pairs becomes more urgent for learning the optimal policy in the true environment. This yields an intrinsic and time-varying robustness–exploration trade-off: robustness is valuable early in learning, but maintaining a fixed conservative attitude can later hinder the exploration needed to learn the true-environment optimal policy. Thus, the interaction policy should adapt its treatment of epistemic uncertainty over time, being more robust when data are scarce and becoming less conservative as information accumulates.

To account for epistemic uncertainty, a widely used approach is robust and distributionally robust MDPs and reinforcement learning, which optimizes worst-case performance over uncertainty or ambiguity sets (Nilim and El Ghaoui 2005, Iyengar 2005, Xu and Mannor 2010, Wiesemann et al. 2013). However, much of this literature focuses on offline settings, where the historical dataset remains fixed throughout learning or data are accessed through a generative model or simulator (Panaganti and Kalathil 2022, Zhou et al. 2021, Panaganti et al. 2022, Blanchet et al. 2023). These results show how robust policies can be learned when data are exogenously available, but do not address how an interaction policy should jointly manage robustness and exploration as data accumulate.

Recent online robust RL works are closer to the present setting (Wang and Zou 2021, Badrinath and Kalathil 2021, Dong et al. 2022, Lu et al. 2024, Wang and Zhou 2023, Ghosh et al. 2026, Wang and Zhou 2025). Some of these studies rely on an external exploratory behavior policy to interact with the true environment (Wang and Zou 2021, Badrinath and Kalathil 2021, Wang and Zhou 2023). However, such a behavior policy does not account for robustness during interaction. Another line of work encourages exploration by adding explicit visit-count-dependent bonuses to robust Bellman backups before selecting the interaction policy (Dong et al. 2022, Lu et al. 2024, Ghosh et al. 2026, Wang and Zhou 2025). These bonuses take larger values early in learning, so exploration can have a greater effect on action selection than the robust value estimate. These methods therefore do not directly ensure that the interaction policy is robust. Moreover, these methods aim to learn an optimal robust policy, whereas our goal is to learn the optimal policy in the true environment while ensuring that the interaction policy is robust, especially early in learning. This leaves open how the interaction policy should adapt its risk attitude over time—being more robust when data are scarce, but becoming less conservative as more data are collected so that the agent can explore enough to learn the optimal policy in the true environment.

The Bayesian risk-aware Markov Decision Process (BR-MDP) provides a starting point to this question. It models unknown parameters in the true environment through a posterior distribution and imposes risk measures on future rewards at each transition step, resulting in a data-adaptive stochastic model (Wu et al. 2018, Lin et al. 2022, Wang and Zhou 2023, Lin and Zhou 2025). Recently, Wang and Zhou (2025) incorporated lower-tail CVaR as the risk measure in the BR-MDP, so that solving the resulting BR-MDP yields a risk-averse policy. Based on this formulation, they proposed an online Bayesian risk-averse algorithm to learn an optimal robust policy under the Bayesian risk criterion. However, its regret analysis also relies on

an additional exploration bonus that is large when visit counts are small. As a result, the interaction policy may not have the desired robustness to epistemic uncertainty early in learning.

To rigorously characterize the robustness-exploration trade-off in online RL, we first study the BR-MDP formulation with a fixed α -quantile as the risk measure, referred to as α -quantile BR-MDP. Our theoretical analysis shows how the α -quantile BR-MDP explicitly controls robustness to epistemic uncertainty while maintaining exploration. The optimal policy of the α -quantile BR-MDP can be more robust or more exploratory, depending on the quantile level α . Therefore, we propose adaptive quantile BR-MDP (AQ-BRMDP), which uses an adaptive quantile schedule to respond to the evolving robustness–exploration trade-off in online RL. Early in learning, the schedule sets the quantile level to emphasize lower-tail evaluations of the cumulative future rewards, yielding a more robust policy. As more data are collected and the posterior concentrates, the schedule gradually increases the quantile level, especially for less-visited state-action pairs that remain important for learning the optimal policy in the true environment, thereby encouraging exploration toward those pairs. In the discounted infinite-horizon setting, we implement this idea through pseudo-episode construction, as in Xu et al. (2024), which partitions the interaction process into intervals with random lengths according to the discount factor. Specifically, at the beginning of each pseudo-episode, we update the posterior belief and quantile schedule, then solve the corresponding α -quantile BR-MDP, and finally execute the resulting policy until the next update. This yields an implementable online procedure that adapts the treatment of epistemic uncertainty to the stage of learning and the collected data.

We summarized the main contributions of this paper as follows.

1. We formulate the α -quantile BR-MDP and show that the quantile level can explicitly control the trade-off between robustness and exploration. We characterize this trade-off through an analytical result that the difference between the value function of the α -quantile BR-MDP and the original value function is asymptotically normal. The magnitude of this mean increases as the quantile level moves farther towards the lower tail, inducing more robust policy, or farther into the upper tail, inducing more exploratory policy. It decreases as more data are collected, at a rate of $O(\frac{1}{\sqrt{N}})$, where N is the total number of data points used to estimate the posterior distribution.
2. We utilize the property above to design an online Bayesian risk-aware algorithm, AQ-BRMDP, that combines adaptive quantile scheduling with pseudo-episodic posterior updates in the discounted infinite-horizon setting. The quantile schedule is designed to depend on both visit counts across state-action pairs and the stage of learning, so AQ-BRMDP can adapt to the evolving robustness–exploration trade-off in online RL settings.
3. Theoretically, we establish that AQ-BRMDP has Bayesian regret bounds of order $\tilde{O}(\sqrt{T})$, where T is the total number of interactions, with respect to two benchmarks: the optimal value in the true environment, and the optimal robust value. Numerically, we evaluate the performance of AQ-BRMDP in two environments: one that requires sustained exploration, and the other in which exploratory mistakes are costly. We also implement an extension of the proposed algorithm to continuous-state spaces and evaluate its empirical performance in a continuous-state environment.

1.1 Related Work

Classical online reinforcement learning studies the exploration–exploitation trade-off for efficiently learning the optimal policy in the true environment. A broad class of optimism-based methods addresses this trade-off through optimistic initialization, optimistic models, confidence sets, or explicit exploration bonuses (Kearns and Singh 2002, Brafman and Tennenholtz 2002, Strehl et al. 2006, Strehl and Littman 2008, Jaksch et al. 2010, Bartlett and Tewari 2009, Azar et al. 2017, He et al. 2021, Jin et al. 2018, Dong et al. 2020). Posterior-sampling methods instead introduce exploration through the randomness of models sampled from

a Bayesian posterior and are typically analyzed through Bayesian regret (Osband et al. 2013, Abbasi-Yadkori and Szepesvári 2015, Russo et al. 2018, Xu et al. 2024). Related posterior-inference and posterior-quantile methods also use posterior information to direct exploration toward actions whose values remain uncertain (Tiapkin et al. 2022, Tarbouriech et al. 2023, Ma and Lee 2026). This literature primarily uses uncertainty to improve learning of the true-environment optimal policy; it does not explicitly control the interaction risk of exploratory actions when epistemic uncertainty is high.

Robust and distributionally robust reinforcement learning originate from robust MDP formulations, where the objective is to optimize performance under worst-case models or over ambiguity sets (Nilim and El Ghaoui 2005, Iyengar 2005, Xu and Mannor 2010, Wiesemann et al. 2013). This line has developed into learning algorithms for generative-model and offline-data settings (Panaganti and Kalathil 2022, Zhou et al. 2021, Panaganti et al. 2022, Blanchet et al. 2023), and more recently into online robust RL with interactive data collection (Wang and Zou 2021, Badrinath and Kalathil 2021, Dong et al. 2022, Lu et al. 2024, Ghosh et al. 2026). These works primarily account for model misspecification and aim to learn robust-optimal policies, but they do not directly address how the behavior policy should balance robustness with the exploration needed to learn the optimal policy in the true environment.

Our work bridges these two lines of work: as robust RL, it accounts for epistemic uncertainty to improve the robustness of the interaction policy; as an online RL method designed for efficient exploration, it ultimately aims to learn the optimal policy in the true environment. The key idea of our work is to use an α -quantile Bayesian risk criterion to interpolate between robustness early in learning and exploration needed later to learn the true-environment optimal policy, rather than treating robustness and exploration as separate mechanisms.

Our paper is built on Bayesian risk optimization and the BRMDP formulation. Bayesian risk optimization was introduced by Zhou and Xie (2015) as a flexible alternative to worst-case robustness in static (one-stage) stochastic optimization, and its statistical properties were established by Wu et al. (2018). This perspective was extended to sequential (multi-stage) decision making through BRMDP, spanning finite- and infinite-horizon formulations as well as offline and online learning settings (Lin et al. 2022, Lin and Zhou 2025, Wang and Zhou 2023, 2025). On a related note, a broader Bayesian RL literature studies how posterior uncertainty can be represented and used in sequential decision making (Ghavamzadeh et al. 2015). In particular, Bayes-adaptive formulations augment the decision state with posterior beliefs and optimize Bayes-adaptive expected return (Duff 2002, Poupart et al. 2006, Ross et al. 2007).

Finally, our paper should be distinguished from safe exploration. In this literature, risk is intrinsic to the true environment, i.e., the possibility that certain actions lead to inherently undesirable outcomes (Garcelon et al. 2020, Yamagata and Santos-Rodríguez 2024). In contrast, the risk we consider does not arise from the environment itself, but from epistemic uncertainty: limited data can cause the agent to act on unreliable estimates of the environment. This risk diminishes as more data are collected.

2 Bayesian Risk-Aware MDPs

2.1 α -quantile Bayesian Risk MDPs

Unknown True Environment. We consider an infinite-horizon discounted Markov decision process (MDP) $\mathcal{M} = (\mathcal{S}, \mathcal{A}, \gamma, r, P^c)$, where \mathcal{S} and \mathcal{A} are finite state and action spaces with $|\mathcal{S}| = S$ and $|\mathcal{A}| = A$, $\gamma \in (0, 1)$ is the discount factor, $r : \mathcal{S} \times \mathcal{A} \rightarrow [0, 1]$ is the reward function, and $P^c(s' | s, a)$ is the true but unknown transition kernel. For notational simplicity, we write $P_{s,a}^c(\cdot) := P^c(\cdot | s, a)$.

Let Π be the set of Markovian policies $\pi = \{\pi_t\}_{t \geq 0}$, where each $\pi_t(\cdot | s)$ is a probability distribution over \mathcal{A} for every $s \in \mathcal{S}$. Given an initial state $s_0 = s$, the objective is to maximize the expected total discounted

reward

$$\sup_{\pi \in \Pi} \mathbb{E}^{\pi} \left[\sum_{t=0}^{\infty} \gamma^t r(s_t, a_t) \mid s_0 = s \right], \quad \forall s \in \mathcal{S}, \quad (1)$$

where $a_t \sim \pi_t(\cdot \mid s_t)$ and $s_{t+1} \sim P^c(\cdot \mid s_t, a_t)$. For a policy $\pi \in \Pi$, the objective function under a fixed policy π in (1) defines the value function of π at state s

$$V^{\pi}(s) := \mathbb{E}^{\pi} \left[\sum_{t=0}^{\infty} \gamma^t r(s_t, a_t) \mid s_0 = s \right], \quad \forall s \in \mathcal{S}. \quad (2)$$

Accordingly, the optimal value function is $V^*(s) := \sup_{\pi \in \Pi} V^{\pi}(s)$, $\forall s \in \mathcal{S}$, and a policy π^* is optimal if $V^{\pi^*}(s) = V^*(s)$ for all $s \in \mathcal{S}$.

For tabular MDPs, there exists a stationary deterministic optimal policy (Puterman 1994). Thus, without loss of optimality, we henceforth restrict attention to stationary deterministic policies of the form $\pi : \mathcal{S} \rightarrow \mathcal{A}$. For any such policy, the value function satisfies the Bellman equation, $\forall s \in \mathcal{S}$,

$$V^{\pi}(s) = r(s, \pi(s)) + \gamma \mathbb{E}_{P_{s, \pi(s)}^c} [V^{\pi}(s')], \quad (3)$$

where $\mathbb{E}_P[V^{\pi}(s')] = \sum_{s' \in \mathcal{S}} P(s') V^{\pi}(s') = P^{\top} V^{\pi}$ is the expected value (EV) of the successor-state value function with respect to the distribution P . The optimal value function V^* satisfies the Bellman optimality equation, $\forall s \in \mathcal{S}$,

$$V^*(s) = \max_{a \in \mathcal{A}} \{r(s, a) + \gamma \mathbb{E}_{P_{s, a}^c} [V^*(s')]\}. \quad (4)$$

In practice, the transition kernel P^c is unknown and must be learned from data, which introduces epistemic uncertainty. We assume throughout that the reward function r is known, but the proposed approach can be extended to settings with unknown rewards.

Bayesian Modeling of the Transition Kernel. To model epistemic uncertainty in the unknown transition kernel P^c , we adopt a Bayesian approach. Specifically, we model each unknown transition vector $P_{s, a}^c$ by a Bayesian random vector $P_{s, a}$ and place independent Dirichlet conjugate priors on $\{P_{s, a}\}_{(s, a) \in \mathcal{S} \times \mathcal{A}}$. After observing a trajectory, the posterior of each $P_{s, a}$ remains Dirichlet by conjugacy, with a parameter vector determined by the prior and the transition counts along the observed trajectory. Details of the Dirichlet definition and posterior update are provided in Appendix EC.1.

When analyzing the BR-MDP under the current posterior, we write $P_{s, a} \sim \text{Dir}(\phi(s, a))$, where $\phi(s, a) = (\phi(s, a, s'))_{s' \in \mathcal{S}}$ is the current posterior parameter vector. We also write $\phi = \{\phi(s, a)\}_{(s, a) \in \mathcal{S} \times \mathcal{A}}$ for the collection of current posterior parameters. The dependence of ϕ on the prior and the observed trajectory is suppressed for notational simplicity in this section.

Bayesian Risk Value Function. To account for epistemic uncertainty represented by the current posterior over transition kernels, we evaluate policies by applying a risk measure with respect to this posterior distribution.

For a policy π , the value function of BR-MDP with posterior parameter ϕ is defined through the Bellman equation (Wang and Zhou 2023, 2025), $\forall s \in \mathcal{S}$,

$$V_{\phi, \alpha}^{\pi}(s) = r(s, \pi(s)) + \gamma \rho_{\phi(s, \pi(s))}^{\alpha}(P^{\top} V_{\phi, \alpha}^{\pi}), \quad (5)$$

where $\rho_{\phi(s, \pi(s))}^{\alpha}(\cdot)$ is a risk measure at level $\alpha \in (0, 1)$ with respect to $\text{Dir}(\phi(s, \pi(s)))$. Notably, the Bayesian risk value function $V_{\phi, \alpha}^{\pi}$ depends on the posterior parameter ϕ . As new data are observed, ϕ is

updated via (EC.1), which changes the posterior distribution of the transition kernel and the associated risk evaluation. Consequently, both the value function and the induced optimal policy evolve over time, reflecting the agent's updated belief about the environment.

As shown by Wang and Zhou (2023, 2025), the value function of BR-MDP also admits an equivalent nested representation:

$$V_{\phi, \alpha}^{\pi}(s_0) = r(s_0, a_0) + \gamma \rho_{\phi(s_0, a_0)}^{\alpha} \left(\mathbb{E}_{P^1} \left[r(s_1, a_1) + \gamma \rho_{\phi(s_1, a_1)}^{\alpha} \left(\mathbb{E}_{P^2} \left[r(s_2, a_2) + \dots \right] \right) \right] \right). \quad (6)$$

where, independently across stages, $P^t \sim \text{Dir}(\phi(s_{t-1}, a_{t-1}))$, $s_t \sim P^t$ for $t \geq 1$, and $a_t = \pi(s_t)$ for $t \geq 0$. Moreover, the optimal value function can be computed via the following Bayesian risk Bellman optimality equation: $\forall s \in \mathcal{S}$,

$$V_{\phi, \alpha}^*(s) = \max_{a \in \mathcal{A}} \left\{ r(s, a) + \gamma \rho_{\phi(s, a)}^{\alpha} (P^{\top} V_{\phi, \alpha}^*) \right\}. \quad (7)$$

By solving (7), we can obtain an optimal policy, $\pi_{\phi, \alpha}^*$, that is deterministic and stationary.

We also define the corresponding Bellman operator under the policy π and the optimal Bellman operator as, $\forall s \in \mathcal{S}$,

$$(\mathcal{T}_{\phi, \alpha}^{\pi} V)(s) := r(s, \pi(s)) + \gamma \rho_{\phi(s, \pi(s))}^{\alpha} (P^{\top} V), \quad (8)$$

$$(\mathcal{T}_{\phi, \alpha}^* V)(s) := \max_{a \in \mathcal{A}} \left\{ r(s, a) + \gamma \rho_{\phi(s, a)}^{\alpha} (P^{\top} V) \right\}. \quad (9)$$

Under structural conditions on the risk measure discussed by Wang and Zhou (2023), $\mathcal{T}_{\phi, \alpha}^{\pi}$ and $\mathcal{T}_{\phi, \alpha}^*$ are γ -contractions under $\|\cdot\|_{\infty}$ and therefore admit unique fixed points.

α -quantile BR-MDP. We specialize the risk measure $\rho^{\alpha}(\cdot)$ to the α -quantile, thereby obtaining an α -quantile BR-MDP. We refer to $V_{\phi, \alpha}^{\pi}$ as the corresponding α -quantile BR-MDP value function. Specifically, for a random variable X and $\alpha \in (0, 1)$, the α -quantile of X is defined as $\rho^{\alpha}(X) := \inf\{z \in \mathbb{R} : \mathbb{P}(X \leq z) \geq \alpha\}$. Under this choice, the quantile level α determines which part of the posterior distribution of $P_{s, a}^{\top} V$ is emphasized in the Bellman backup, thereby encoding a risk attitude toward epistemic uncertainty.

To illustrate the effect of the quantile level α , we define the one-step adjustment induced by replacing the true EV of successor states with its posterior α -quantile as follows:

$$b_{\phi(s, a)}^{\alpha}(V) := \rho_{\phi(s, a)}^{\alpha}(P^{\top} V) - \mathbb{E}_{P_{s, a}^c} [V(s')].$$

The optimal Bellman operator can then be written as

$$(\mathcal{T}_{\phi, \alpha}^* V)(s) = \max_{a \in \mathcal{A}} \left\{ r(s, a) + \gamma \mathbb{E}_{P_{s, a}^c} [V(s')] + \gamma b_{\phi(s, a)}^{\alpha}(V) \right\}, \quad \forall s \in \mathcal{S}.$$

This representation decomposes the Bellman backup into $r(s, a) + \gamma \mathbb{E}_{P_{s, a}^c} [V(s')]$, the backup under the true transition kernel for (s, a) , and the one-step adjustment $b_{\phi(s, a)}^{\alpha}(V)$ that captures both the risk attitude and the belief about epistemic uncertainty in the transition kernel.

We next briefly discuss how the risk level α and the posterior parameter ϕ together affect the optimal policy from a **Bayesian perspective**. Conditional on the current posterior parameter $\phi(s, a)$, the unknown true transition vector $P_{s, a}^c$ is viewed as a draw from the posterior $\text{Dir}(\phi(s, a))$ and $b_{\phi(s, a)}^{\alpha}(V) = \rho_{\phi(s, a)}^{\alpha}(P^{\top} V) - (P_{s, a}^c)^{\top} V$. Therefore, by the definition of the α -quantile, the posterior probability of $b_{\phi(s, a)}^{\alpha}(V) \geq 0$ is at least α . For large α , the Bellman backup in (7) emphasizes the upper tail of the posterior distribution of $P_{s, a}^{\top} V$. In this case, $b_{\phi(s, a)}^{\alpha}(V)$ is positive with high posterior probability α and acts as an implicit bonus for exploration, reflecting an optimistic attitude toward epistemic uncertainty about the transition kernel.

Moreover, for such large α , the magnitude of $b_{\phi(s,a)}^\alpha(V)$ increases with larger epistemic uncertainty (i.e., a more dispersed posterior distribution of $P_{s,a}$). Therefore, $b_{\phi(s,a)}^\alpha(V)$ acts as an exploration incentive for state-action pairs (s, a) with high epistemic uncertainty about $P_{s,a}$. Conversely, when α is small, $b_{\phi(s,a)}^\alpha(V)$ is negative with high posterior probability $1 - \alpha$ and its magnitude increases with larger epistemic uncertainty. As a result, the one-step adjustment $b_{\phi(s,a)}^\alpha(V)$ acts as an implicit penalty for epistemic uncertainty about $P_{s,a}$ and thereby yields a policy that is more robust to epistemic uncertainty.

Overall, when $b_{\phi(s,a)}^\alpha(V)$ is positive, it plays a role analogous to an optimistic exploration bonus in online RL methods such as UCBVI- γ (He et al. 2021), but it is induced by the posterior quantile rather than added as an explicit term derived by concentration inequalities. This adjustment can also be negative when the quantile level is chosen in the lower tail, therefore acting as a pessimistic penalty.

2.2 Asymptotic Analysis of α -quantile BR-MDP

In the previous subsection, we introduced α -quantile BR-MDP to account for epistemic uncertainty in the unknown transition kernel and discussed how the quantile level α reflects a risk attitude toward this uncertainty. In this subsection, we further refine this interpretation by studying the asymptotic behavior of the gap between the α -quantile BR-MDP value function $V_{\phi,\alpha}^\pi$ and the true value function V^π as the Dirichlet posterior concentrates. Let $P_\pi^c := (P_{s,\pi(s)}^c)_{s \in \mathcal{S}}$ denote the true transition matrix induced by policy π , and let $\text{diag}(x)$ denote the diagonal matrix with diagonal entries given by the entries of x . We impose the following regularity conditions on the data-collection scheme.

Assumption 1. Fix a stationary deterministic policy π .

- (i) Let N denote the total number of observed transitions. The data are collected along an on-policy trajectory $\{s_0, a_0, s_1, \dots, s_{N-1}, a_{N-1}, s_N\}$, where $a_i = \pi(s_i)$ and $s_{i+1} \sim P_{s_i, a_i}^c$ for $i = 0, \dots, N-1$. Define the visit count of each state-action pair by $N(s, a) := \sum_{i=0}^{N-1} \mathbb{I}\{s_i = s, a_i = a\}$. For each $s \in \mathcal{S}$, there exists a constant $\bar{n}_s \in (0, 1)$ such that

$$\frac{N(s, \pi(s))}{N} \xrightarrow{\text{a.s.}} \bar{n}_s, \quad \sum_{s \in \mathcal{S}} \bar{n}_s = 1.$$

- (ii) For each state-action pair $(s, a) \in \mathcal{S} \times \mathcal{A}$, the prior on $P_{s,a}$ is a uniform Dirichlet prior with $\phi_0(s, a, s') = 1, \forall s' \in \mathcal{S}$.

Assumption 1(i) is a trajectory-based sampling condition. It is weaker than the state-action-wise independent sampling condition used in Wang and Zhou (2025), which assumes independent transition samples within each state-action pair and mutual independence across different state-action pairs. Here, the data are collected along a single on-policy trajectory, and the induced temporal dependence is handled in the proof by a martingale central limit theorem (CLT). The ratio condition ensures that each on-policy state-action pair $(s, \pi(s))$ receives a nonvanishing fraction of the total number of observations; it holds, for instance, when the Markov chain induced by P_π^c is ergodic with a strictly positive stationary mass on every state. Assumption 1(ii) is used only for notational simplicity. More generally, any fixed Dirichlet prior with strictly positive parameters contributes only $O(1)$ pseudo-counts and therefore does not affect the limiting behavior.

Theorem 1 (Asymptotic normality for α -quantile BR-MDP). *Fix $\alpha \in (0, 1)$ and let $z_\alpha := \Phi^{-1}(\alpha)$, where Φ is the cdf of the standard normal distribution. Under Assumption 1,*

$$\sqrt{N} (I - \gamma P_\pi^c) (V_{\phi,\alpha}^\pi - V^\pi) \Rightarrow \mathcal{N}(\gamma \lambda_\pi, \text{diag}((\gamma \sigma_\pi)^2)),$$

where, for each $s \in \mathcal{S}$, $\sigma_\pi^2(s) := \frac{1}{\bar{n}_s} \text{Var}_{s' \sim P_{s,\pi(s)}^c} [V^\pi(s')]$, and $\lambda_\pi(s) := z_\alpha \sigma_\pi(s)$.

The proof of Theorem 1 is deferred to Appendix EC.2. In particular, Theorem 1 yields the following expansion of the α -quantile BR-MDP value function:

$$V_{\phi, \alpha}^{\pi} = V^{\pi} + (I - \gamma P_{\pi}^c)^{-1} \times \left(\frac{\gamma \lambda_{\pi}}{\sqrt{N}} + \frac{\gamma \operatorname{diag}(\sigma_{\pi}) Z}{\sqrt{N}} \right) + o_p(N^{-1/2}), \quad (10)$$

where $\sigma_{\pi} := (\sigma_{\pi}(s))_{s \in \mathcal{S}}$, $o_p(\cdot)$ denotes little- o notation in probability with respect to the randomness of the observed data, and $Z \sim \mathcal{N}(0, I_S)$ is a standard multivariate normal vector. For fixed $\alpha \in (0, 1)$, (10) yields a stochastic expansion of $V_{\phi, \alpha}^{\pi}$ around V^{π} , whose leading term decomposes into a deterministic bias term of order $N^{-1/2}$ and a Gaussian fluctuation term, with remainder $o_p(N^{-1/2})$. More specifically, before Bellman propagation, i.e., before multiplying by $(I - \gamma P_{\pi}^c)^{-1}$ in (10), the asymptotic mean of the one-step adjustment $b_{\phi(s, \pi(s))}^{\alpha}(V^{\pi})$ is given by

$$\frac{\lambda_{\pi}(s)}{\sqrt{N}} = z_{\alpha} \sqrt{\frac{\operatorname{Var}_{s' \sim P_{s, \pi(s)}^c} [V^{\pi}(s')]}{\bar{n}_s N}}. \quad (11)$$

The magnitude of (11) is larger for states that are sampled less frequently (i.e. small \bar{n}_s) or for which the next-state value $V^{\pi}(s')$ is more dispersed under the true transition kernel (i.e. large $\operatorname{Var}_{s' \sim P_{s, \pi(s)}^c} [V^{\pi}(s')]$). The sign of (11) is determined by z_{α} : when $\alpha < 0.5$, the asymptotic mean of the one-step adjustment is negative, so it discourages visiting less frequently visited states on average, reflecting a conservative attitude toward epistemic uncertainty and inducing an underestimation of $V_{\phi, \alpha}^{\pi}$ after Bellman propagation; when $\alpha = 0.5$, $z_{0.5} = 0$, so the deterministic bias term in the asymptotic expansion vanishes. This makes the 0.5-quantile BR-MDP asymptotically risk-neutral, similar to applying the posterior expectation in (5) under the normal approximation; when $\alpha > 0.5$, z_{α} becomes positive, so the one-step adjustment provides a bonus to visit less frequently visited states on average, encouraging exploration, reflecting an optimistic attitude and inducing an overestimation due to such exploration incentives. Thus, Theorem 1 shows how the quantile level α of the quantile BR-MDP accounts for epistemic uncertainty in the asymptotic regime.

The matrix $(I - \gamma P_{\pi}^c)^{-1}$ then propagates this one-step adjustment through state transitions. For fixed N , the deterministic component in (10), $(I - \gamma P_{\pi}^c)^{-1} \gamma \lambda_{\pi} / \sqrt{N}$, represents the mean shift of $V_{\phi, \alpha}^{\pi}$ away from V^{π} induced by the α -quantile in the Bellman backup. Since $\lambda_{\pi} = z_{\alpha} \sigma_{\pi} \rightarrow \pm \infty$ as $\alpha \uparrow 1$ or $\alpha \downarrow 0$, the magnitude of the mean shift increases as the quantile level moves farther into the upper tail for exploration or farther into the lower tail for robustness. On the other hand, for every fixed $\alpha \in (0, 1)$, since $\|(I - \gamma P_{\pi}^c)^{-1}\|_{\infty} \leq (1 - \gamma)^{-1}$, the deterministic component $(I - \gamma P_{\pi}^c)^{-1} \gamma \lambda_{\pi} / \sqrt{N}$ is bounded in sup-norm by $\frac{\gamma}{1 - \gamma} |z_{\alpha}| \|\sigma_{\pi}\|_{\infty} / \sqrt{N}$. Hence, the mean shift induced by a fixed quantile level α shrinks automatically as more data are collected, which implies that the trade-off between robustness and exploration diminishes with more data. As a result, for every fixed $\alpha \in (0, 1)$, the difference $V_{\phi, \alpha}^{\pi} - V^{\pi}$ is of order $O_p(N^{-1/2})$.

Finally, the asymptotic covariance σ_{π}^2 in Theorem 1 does not depend on α . Thus, α only controls the direction and magnitude of the mean shift, whereas the intrinsic variability is determined by the true transition dynamics and the policy used.

2.3 Finite-sample Robustness of α -quantile BR-MDP

In the previous subsection, we introduced α -quantile BR-MDP to account for epistemic uncertainty in the unknown transition kernel and discussed how the quantile level α reflects a risk attitude toward this uncertainty. In this subsection, we further provide a robustness interpretation of α -quantile BR-MDP.

With a slight abuse of notation, let $P = (P_{s,a})_{(s,a) \in \mathcal{S} \times \mathcal{A}}$ be the random transition kernel obtained by independently drawing $P_{s,a} \sim \operatorname{Dir}(\phi(s, a))$ for each state-action pair. Let \mathbb{P}_{ϕ} denote the posterior probability measure over the transition kernel P and $\rho_{\phi}^{\alpha}(\cdot)$ denote the α -quantile with respect to the transition kernel P .

Given a realized transition kernel P and a policy π , let V_P^π denote the value function of π under the transition kernel P . For each state $s \in \mathcal{S}$, we define the posterior α -quantile value of policy π by

$$V_{\phi,\alpha}^{\pi,q}(s) := \sup \left\{ c \in \mathbb{R} : \mathbb{P}_\phi(V_P^\pi(s) \geq c) \geq 1 - \alpha \right\}. \quad (12)$$

Thus, $V_{\phi,\alpha}^{\pi,q}(s)$ is the largest value threshold that $V_P^\pi(s)$ exceeds with posterior probability at least $1 - \alpha$. Smaller values of α correspond to a stronger robustness guarantee.

Assume that, for every fixed policy π and state s , the posterior distribution of $V_P^\pi(s)$ is continuous, then $V_{\phi,\alpha}^{\pi,q}(s) = \rho_\phi^\alpha(V_P^\pi(s))$. Here, $\rho_\phi^\alpha(V_P^\pi(s))$ applies the risk measure to the entire value function V_P^π , rather than applying the risk measure at each transition stage, as in the nested formulation of $V_{\phi,\alpha}^\pi$ in (6). Since the quantile functional is non-additive, $V_{\phi,\alpha}^{\pi,q}$ does not admit a Bellman equation in general. The hardness results of Delage and Mannor (2010) imply that directly optimizing the corresponding posterior quantile objective, i.e. $\max_\pi V_{\phi,\alpha}^{\pi,q}(s)$, is NP-hard under general uncertainty in the transition parameters. Even under independent Dirichlet transition priors, exact optimization remains difficult. Instead, α -quantile BR-MDP value function can serve as a tractable lower bound, as shown in the following proposition.

Proposition 1. *For $\alpha \in (0, 1)$, let $\bar{\alpha} := 1 - (1 - \alpha)^{1/S}$. Assume that, for every fixed policy π and state s , the posterior distribution of $V_P^\pi(s)$ is continuous. For any fixed policy π ,*

$$\mathbb{P}_\phi \left(V_P^\pi(s) \geq V_{\phi,\bar{\alpha}}^\pi(s), \quad \forall s \in \mathcal{S} \right) \geq 1 - \alpha.$$

Consequently, for every $s \in \mathcal{S}$, $V_{\phi,\alpha}^{\pi,q}(s) \geq V_{\phi,\bar{\alpha}}^\pi(s)$.

The proof of Proposition 1 is in Appendix EC.3. As an immediate consequence, for any fixed state s , $\max_\pi V_{\phi,\alpha}^{\pi,q}(s) \geq \max_\pi V_{\phi,\bar{\alpha}}^\pi(s)$. Thus, maximizing the $\bar{\alpha}$ -quantile value function gives a conservative surrogate for maximizing the posterior α -quantile value. Proposition 1, together with (12), shows that, for small α , α -quantile BR-MDP admits a finite-sample robustness interpretation: the posterior α -quantile value $V_{\phi,\alpha}^{\pi,q}$ provides a posterior high-probability $(1 - \alpha)$ performance guarantee, and the nested $\bar{\alpha}$ -quantile BR-MDP value $V_{\phi,\bar{\alpha}}^\pi$ is a tractable lower bound for this robustness guarantee.

3 Online RL via Adaptive Quantile Scheduling

Section 2 showed that the quantile level in α -quantile BR-MDP provides a flexible way to handle epistemic uncertainty captured by the posterior distribution for different purposes, namely robustness and exploration. We now turn to the online setting, where this flexibility becomes algorithmically useful for adapting to the evolving robustness–exploration trade-off over the course of learning. To illustrate such a trade-off, two examples that separately demonstrate the robustness and exploration sides of this trade-off are presented in Section EC.4. Section 3.1 introduces an adaptive quantile schedule that tracks this evolving trade-off by varying the quantile level across learning stages and across state-action pairs. Then, Section 3.2 embeds this mechanism into a pseudo-episode scheme for discounted infinite-horizon problems, enabling a fully online learning algorithm. Specifically, at the start of each pseudo-episode, we update the posterior, compute the quantile level, solve the corresponding α -quantile BR-MDP, and then execute the resulting policy to collect more data until the next update.

3.1 Adaptive Quantile Scheduling

To track the evolving robustness–exploration trade-off identified in Section EC.4, we let the quantile level vary across pseudo-episodes and across state-action pairs.

We index the pseudo-episodes by $k = 1, 2, \dots$. At the beginning of the k th pseudo-episode, for each $(s, a) \in \mathcal{S} \times \mathcal{A}$, let $N_k(s, a, s')$ denote the number of transitions from (s, a) to s' , and let $N_k(s, a) := \sum_{s' \in \mathcal{S}} N_k(s, a, s')$ denote the total number of visits to (s, a) . Under the prior $\text{Dir}(1, \dots, 1)$, for each (s, a) , the posterior distribution of $P_{s,a}$ at pseudo-episode k is denoted by $\text{Dir}(\phi_k(s, a))$ and the posterior parameters are updated as follows:

$$\phi_k(s, a, s') = 1 + N_k(s, a, s'), \quad \phi_k(s, a) = (\phi_k(s, a, s'))_{s' \in \mathcal{S}}. \quad (13)$$

Let $\phi_k = \{\phi_k(s, a)\}_{(s,a) \in \mathcal{S} \times \mathcal{A}}$ denote the collection of posterior parameters at the beginning of the k th pseudo-episode. To construct the adaptive quantile schedule, we first define the adjusted visit count and its average by $N_k^+(s, a) := \max\{N_k(s, a), 1\}$, and $\bar{N}_k^+ := \frac{1}{SA} \sum_{(s,a) \in \mathcal{S} \times \mathcal{A}} N_k^+(s, a)$. The relative visit count of (s, a) is then defined as

$$r_k(s, a) := \frac{N_k^+(s, a)}{\bar{N}_k^+}, \quad (s, a) \in \mathcal{S} \times \mathcal{A},$$

which compares the number of visits to (s, a) with the average adjusted visit count over the state-action space. We also define the scaling factor:

$$g_k := \frac{\ln(2k)}{\sqrt{k}},$$

whose scaling form is chosen in accordance with the regret guarantee established in Section 4.

Given a problem-specified robustness target parameter $\underline{\alpha} \in (0, 1)$, which encodes the degree of lower-tail robustness that the decision maker deems sufficient when acting under epistemic uncertainty, and an algorithmic sensitivity parameter $\delta > 0$, we define the adaptive quantile schedule as follows:

$$\alpha_k(s, a) = \max\{1 - \delta r_k(s, a) g_k, \underline{\alpha}\}. \quad (14)$$

Before explaining the intuition behind the schedule (14), we extend the formulation of the α -quantile BR-MDP with a common quantile level α across all state-action pairs to allow state-action-dependent quantile levels. Specifically, let $\alpha : \mathcal{S} \times \mathcal{A} \rightarrow (0, 1)$ and replace $\rho_{\phi(s_t, a_t)}^\alpha$ in (6) with $\rho_{\phi(s_t, a_t)}^{\alpha(s_t, a_t)}$. With a slight abuse of notation, we write $\alpha = (\alpha(s, a))_{(s,a) \in \mathcal{S} \times \mathcal{A}}$ and use $\rho_{\phi(s, a)}^\alpha$ as shorthand for $\rho_{\phi(s, a)}^{\alpha(s, a)}$. With this notation, the Bellman equations (5)–(7) and the Bellman operators (8)–(9) retain exactly the same form in the state-action-dependent case. Moreover, under the same structural conditions on the risk measure as in Section 2, the corresponding Bellman operators remain γ -contractions under $\|\cdot\|_\infty$ and therefore admit unique fixed points.

The factor g_k in (14) depends only on k and controls how far the quantile levels are pushed toward the lower tail across different pseudo-episodes. Early in learning, before visit counts become highly imbalanced across state-action pairs, $r_k(s, a)$ typically does not vary much across state-action pairs, whereas the common factor g_k is relatively large in the early pseudo-episodes. Accordingly, the quantile levels $\alpha_k(s, a)$ remain in the lower-tail regime, so the Bellman backup of the corresponding quantile BR-MDP focuses on lower-tail performance of the EV of successor states and therefore yields a more robust policy as discussed in Section 2.

This robustness is not uniform across state-action pairs. The factor $r_k(s, a)$ adjusts the quantile level according to relative visit counts. Before the floor $\underline{\alpha}$ becomes binding, a less-visited (s, a) pair has a smaller $r_k(s, a)$ and thus a larger $\alpha_k(s, a)$. Consequently, in the Bellman backup for such (s, a) , the EV of successor states is evaluated at a less extreme lower quantile level. This effect is not confined to the local state-action pair but propagates backward to states from which this less-visited pair can be reached through repeated Bellman backups.

As k increases, the common factor g_k decreases and visit counts $N_k(s, a)$ can become imbalanced across (s, a) . Consequently, $r_k(s, a)g_k$ may become sufficiently small for less-visited (s, a) pairs, causing the schedule to move the quantile level $\alpha_k(s, a)$ toward the upper tail and thereby encouraging exploration of

these less-visited pairs, as discussed in Section 2. Moreover, in (14), δ controls the sensitivity of the schedule to relative visit counts.

3.2 Pseudo-Episodes and Algorithm

In finite-horizon MDPs, it is natural to update the posterior and recompute the policy at the beginning of each episode (Osband et al. 2013, Osband and Van Roy 2016). In the discounted infinite-horizon setting considered here, however, no natural episodes are available. Updating the posterior and recomputing the policy after every transition would be computationally demanding, whereas long deterministic artificial episodes may delay the use of newly collected data. We therefore partition the interaction stream into pseudo-episodes, as in Xu et al. (2024).

For each $t \geq 1$, after observing the transition at time t , we draw an independent pseudo-episode indicator $X_{t+1} \sim \text{Bernoulli}(\gamma)$, and interpret $X_{t+1} = 1$ as continuing the current pseudo-episode and $X_{t+1} = 0$ as starting a new pseudo-episode at time $t + 1$. We initialize $X_1 = 0$, so that time 1 starts the first pseudo-episode. Then, the pseudo-episode length L follows a Geometric distribution with parameter $1 - \gamma$ on $\{1, 2, \dots\}$, denoted by $L \sim \text{Geom}(1 - \gamma)$, and is independent of the trajectory. With such a random length, the expectation of the accumulated reward with respect to L is equal to the discounted accumulated reward, i.e. for any realized reward sequence $\{r(s_i, a_i)\}_{i \geq 0}$ indexed from the start of the pseudo-episode,

$$\mathbb{E}_{L \sim \text{Geom}(1-\gamma)} \left[\sum_{i=0}^{L-1} r(s_i, a_i) \right] = \sum_{i=0}^{\infty} \mathbb{P}(L \geq i+1) r(s_i, a_i) = \sum_{i=0}^{\infty} \gamma^i r(s_i, a_i).$$

Let K_T denote the number of pseudo-episodes started by time T , and hence $\mathbb{E}[K_T] = 1 + (T-1)(1-\gamma)$. Hence, the expected number of pseudo-episodes, which is equivalent to the number of posterior updates and policy recomputations, grows on the order of $(1-\gamma)T$ rather than T .

Let $\mathcal{H}_t := \{(s_\tau, a_\tau, s_{\tau+1})\}_{\tau=1}^{t-1}$ denote the interaction history available before time t . By incorporating the adaptive quantile schedule with the pseudo-episodic posterior updates, we obtain the Adaptive Quantile BR-MDP (AQ-BRMDP), summarized in Algorithm 1.

Algorithm 1 AQ-BRMDP

- 1: **Input:** Discount factor γ , total learning time T , schedule parameters δ and $\underline{\alpha}$
 - 2: Initialize $t \leftarrow 1$, $k \leftarrow 0$, $X_1 \leftarrow 0$, and $\mathcal{H}_1 \leftarrow \emptyset$
 - 3: **while** $t \leq T$ **do**
 - 4: **if** $X_t = 0$ **then**
 - 5: $k \leftarrow k + 1$ and $t_k \leftarrow t$
 - 6: Update the posterior ϕ_k using \mathcal{H}_{t_k} according to (13)
 - 7: Compute $\alpha_k(s, a)$ for all $(s, a) \in \mathcal{S} \times \mathcal{A}$ via (14)
 - 8: Compute π_k by solving the α_k -quantile BR-MDP under ϕ_k via value iteration (Algorithm EC.1 in Appendix EC.5)
 - 9: **end if**
 - 10: Take action $a_t \leftarrow \pi_k(s_t)$ and observe the next state s_{t+1}
 - 11: Update the history $\mathcal{H}_{t+1} \leftarrow \mathcal{H}_t \cup \{(s_t, a_t, s_{t+1})\}$
 - 12: **if** $t < T$ **then**
 - 13: Sample $X_{t+1} \sim \text{Bernoulli}(\gamma)$
 - 14: **end if**
 - 15: $t \leftarrow t + 1$
 - 16: **end while**
-

4 Regret Analysis

Section 3 introduced the adaptive quantile schedule and its pseudo-episodic implementation to account for the evolving robustness–exploration trade-off in online learning. We now establish performance guarantees for AQ-BRMDP. We analyze Bayesian regret relative to two complementary benchmarks. The first benchmark is the true-optimal value V^* , which measures regret relative to the optimal value function in the true environment. The second benchmark is the robust-optimal value in the k th pseudo-episode $V_{\phi_k, \underline{\alpha}}^*$, which measures regret relative to the optimal value function of the $\underline{\alpha}$ -quantile BR-MDP under posterior parameters ϕ_k . In implementation, the quantiles are approximated by sampling transition kernels from the posterior distribution, and the corresponding quantile BR-MDP is solved in the simulator. Compared with the cost of interacting with the true environment, the computational cost of posterior sampling and solving the quantile BR-MDP is treated as negligible. Accordingly, we assume that the policy computed in each pseudo-episode can be made arbitrarily close to the exact optimal policy of the corresponding quantile BR-MDP, and we ignore the resulting approximation error in the regret analysis.

Throughout this section, $s_{k,i}$ denotes the state at the i th time step of pseudo-episode k , $\pi_k = \pi_{\phi_k, \underline{\alpha}}^*$ is the policy executed in pseudo-episode k , $V_k := V_{\phi_k, \alpha_k}^*$ denotes the optimal value of the corresponding adaptive α_k -quantile BR-MDP, and L_k denotes the realized length of pseudo-episode k within the interaction horizon T . Bayesian regret (BR) relative to the true-optimal benchmark is defined by

$$BR(T) := \mathbb{E} \left[\sum_{k=1}^{K_T} \sum_{i=1}^{L_k} \left(V^*(s_{k,i}) - V^{\pi_k}(s_{k,i}) \right) \right], \quad (15)$$

where the expectation is taken over the prior distribution of the true transition kernel, the trajectory randomness, and the randomness of the pseudo-episode lengths. To quantify whether exploration incurs substantial loss relative to a conservative benchmark, we also define Bayesian regret relative to the robust-optimal benchmark (BR-R) as follows:

$$BR-R(T) := \mathbb{E} \left[\sum_{k=1}^{K_T} \sum_{i=1}^{L_k} \left(V_{\phi_k, \underline{\alpha}}^*(s_{k,i}) - V^{\pi_k}(s_{k,i}) \right) \right], \quad (16)$$

where the expectation is taken over the prior distribution of the true transition kernel, the trajectory randomness, and the randomness of the pseudo-episode lengths. Let \mathcal{F}_t denote the sigma-field generated by the interaction history and the pseudo-episode indicators observed before time t : $\mathcal{F}_t := \sigma\left((s_\tau, a_\tau, s_{\tau+1})_{\tau=1}^{t-1}, X_1, \dots, X_t\right)$.

Lemma 1 (Dual-benchmark optimism). *Fix pseudo-episode k with starting time t_k . Then:*

- (i) $\mathbb{P}(\forall s \in \mathcal{S} : V^*(s) \leq V_k(s) \mid \mathcal{F}_{t_k}) \geq 1 - \frac{\delta SA \ln(2k)}{\sqrt{k}}$.
- (ii) $V_{\phi_k, \underline{\alpha}}^*(s) \leq V_k(s), \quad \forall s \in \mathcal{S}$.

We defer the proof of Lemma 1 to Appendix EC.6.1. Part (i) in Lemma 1 shows that the true optimal value function V^* can be upper bounded by V_k with posterior probability tending to 1 as learning progresses (i.e., as k increases). Part (ii) in Lemma 1 shows that the robust-optimal value function $V_{\phi_k, \underline{\alpha}}^*$ can also be upper bounded by V_k for every state s .

Define the optimistic event $\mathcal{G}_k := \bigcap_{(s,a) \in \mathcal{S} \times \mathcal{A}} \left\{ (P_{s,a}^c)^\top V_k \leq \rho_{\phi_k(s,a)}^{\alpha_k} (P^\top V_k) \right\}$, which is the event that the BR-MDP EV overestimates the true EV. We show that on \mathcal{G}_k , $V^*(s) \leq V_k(s)$ for all $s \in \mathcal{S}$ in Appendix EC.6.1. Hence, we can decompose the upper bound for $BR(T)$ in (15) before taking expectations as follows:

$$\sum_{k=1}^{K_T} \sum_{i=1}^{L_k} \left(V^*(s_{k,i}) - V^{\pi_k}(s_{k,i}) \right) \leq \sum_{k=1}^{K_T} \sum_{i=1}^{L_k} \left(V_k(s_{k,i}) - V^{\pi_k}(s_{k,i}) \right) + \frac{1}{1-\gamma} \sum_{k=1}^{K_T} L_k \mathbb{I}\{\mathcal{G}_k^c\}. \quad (17)$$

Using Lemma 1 (ii), we can decompose the corresponding upper bound for $BR-R(T)$ in (16) as follows:

$$\sum_{k=1}^{K_T} \sum_{i=1}^{L_k} \left(V_{\phi_k, \underline{\alpha}}^*(s_{k,i}) - V_{\phi_k, \underline{\alpha}}^{\pi_k}(s_{k,i}) \right) \leq \sum_{k=1}^{K_T} \sum_{i=1}^{L_k} \left(V_k(s_{k,i}) - V_{\phi_k, \underline{\alpha}}^{\pi_k}(s_{k,i}) \right). \quad (18)$$

Therefore, the main remaining terms to control are the value-difference terms in (17) and (18), together with the non-optimistic-event term in (17). The next lemma shows that the gap between the value of a fixed policy in the true environment V^π and the value of α_k -quantile BR-MDP under the posterior distribution with parameters ϕ_k , V_{ϕ_k, α_k}^π , can be expressed as the cumulative one-step discrepancy between the α_k -quantile BR-MDP Bellman backup and the corresponding Bellman backup under the true transition along the realized trajectory.

Lemma 2 (Pseudo-episode value decomposition). *Fix pseudo-episode k with starting time t_k , and fix a stationary deterministic policy π . Let $\{(s_{k,i}, a_{k,i})\}_{i \geq 1}$ be the infinite-horizon trajectory generated by following π from time t_k in the true MDP, so that $a_{k,i} := \pi(s_{k,i})$ for all $i \geq 1$. Define $E_{k,i} := \rho_{\phi_k(s_{k,i}, a_{k,i})}^{\alpha_k} (P^\top V_{\phi_k, \alpha_k}^\pi) - (P_{s_{k,i}, a_{k,i}}^c)^\top V_{\phi_k, \alpha_k}^\pi$, $i \geq 1$.*
Then

$$\mathbb{E} \left[\sum_{i=1}^{L_k} \left(V_{\phi_k, \alpha_k}^\pi(s_{k,i}) - V^\pi(s_{k,i}) \right) \middle| \mathcal{F}_{t_k}, P^c \right] = \mathbb{E} \left[\sum_{i=1}^{L_k} i \gamma E_{k,i} \middle| \mathcal{F}_{t_k}, P^c \right]. \quad (19)$$

Here the conditional expectation is taken over the trajectory randomness under π in the true MDP and the independent pseudo-episode lengths $\{L_k : k \geq 1\}$.

The proof of Lemma 2 is deferred to Appendix EC.6.2. For the robust regret, the following lemma provides an analogous decomposition between the α_k -quantile BR-MDP value function and the $\underline{\alpha}$ -quantile BR-MDP value function.

Lemma 3. *Fix pseudo-episode k with starting time t_k , and fix a stationary deterministic policy π . Let $\{(s_{k,i}, a_{k,i})\}_{i \geq 1}$ be the infinite-horizon trajectory generated by following π from time t_k in the true environment, so that $a_{k,i} := \pi(s_{k,i})$ for all $i \geq 1$. Define $E_{k,i}^- := (P_{s_{k,i}, a_{k,i}}^c)^\top V_{\phi_k, \underline{\alpha}}^\pi - \rho_{\phi_k(s_{k,i}, a_{k,i})}^{\underline{\alpha}} (P^\top V_{\phi_k, \underline{\alpha}}^\pi)$, and $E_{k,i} := \rho_{\phi_k(s_{k,i}, a_{k,i})}^{\alpha_k} (P^\top V_{\phi_k, \alpha_k}^\pi) - (P_{s_{k,i}, a_{k,i}}^c)^\top V_{\phi_k, \alpha_k}^\pi$. Then*

$$\mathbb{E} \left[\sum_{i=1}^{L_k} \left(V_{\phi_k, \alpha_k}^\pi(s_{k,i}) - V_{\phi_k, \underline{\alpha}}^\pi(s_{k,i}) \right) \middle| \mathcal{F}_{t_k}, P^c \right] = \mathbb{E} \left[\sum_{i=1}^{L_k} i \gamma (E_{k,i} + E_{k,i}^-) \middle| \mathcal{F}_{t_k}, P^c \right]. \quad (20)$$

Here the conditional expectation is taken over the trajectory randomness under π in the true environment and the independent pseudo-episode lengths $\{L_k : k \geq 1\}$.

Using Lemmas 1 to 3 together with Dirichlet-posterior concentration in Lemma 9, we upper bound the Bayesian regret of AQ-BRMDP under both benchmarks.

Theorem 2. *Suppose that the schedule parameter δ in (14) satisfies $\delta > 0$. If $T \geq S^2 A$, then*

$$BR(T) \leq \tilde{O} \left(\frac{\gamma \sqrt{S A T \ln \frac{e}{1-\alpha}}}{(1-\gamma)^2} + \frac{\delta S A \sqrt{T}}{(1-\gamma)^2} + \frac{S A}{(1-\gamma)^3} \right),$$

and

$$BR-R(T) \leq \tilde{O} \left(\frac{\gamma \sqrt{S A T \ln \frac{1}{\min\{1-\alpha, \alpha\}}}}{(1-\gamma)^2} + \frac{S A}{(1-\gamma)^3} \right),$$

where $\tilde{O}(\cdot)$ suppresses polylogarithmic factors in S , A , T , $1/\delta$, and $1/(1-\gamma)$.

Theorem 2 formalizes that the adaptive schedule accounts for the evolving robustness–exploration trade-off described in Section 3. For fixed problem parameters, the Bayesian regret bound for AQ-BRMDP grows as $\tilde{O}(\sqrt{T})$ in the total number of interactions T . The term $\delta SA\sqrt{T}/(1-\gamma)^2$ captures the additional regret associated with using a more robust interaction policy early in learning. Choosing a larger constant δ would strengthen early robustness, at the cost of a larger $\delta SA\sqrt{T}/(1-\gamma)^2$ term in the regret bound. If the focus is on the standard exploration–exploitation trade-off rather than on prioritizing additional early-stage robustness, we can set $\delta = 1/\sqrt{SA}$. This choice keeps the robustness-induced regret term at the same order as the first term, $\sqrt{SAT}/(1-\gamma)^2$, in its dependence on S , A , T , and $(1-\gamma)^{-1}$ up to the explicit factor $\gamma\sqrt{\ln(e/(1-\underline{\alpha}))}$ and polylogarithmic factors hidden in $\tilde{O}(\cdot)$. The T -independent lower-order term $SA/(1-\gamma)^3$ comes from the finite-time analysis of the pseudo-episode construction for discounted infinite-horizon learning. When $T \geq SA \max\{S, 1/(1-\gamma)^2\}$, this lower-order term is absorbed by the \sqrt{T} terms, so the dominant scaling becomes $\tilde{O}(\sqrt{SAT}/(1-\gamma)^2)$. Thus, with this choice of δ , AQ-BRMDP achieves the same Bayesian regret rate as state-of-the-art Bayesian RL algorithms, such as the $\tilde{O}(H\sqrt{SAT})$ bound for posterior sampling in RL (PSRL) (Osband and Van Roy 2017), up to logarithmic and horizon-dependent factors.

The difference in horizon dependence stems from the different definitions of Bayesian regret in finite-horizon episodic and discounted infinite-horizon settings. Finite-horizon episodic PSRL bounds $\tilde{O}(H\sqrt{SAT})$ are typically expressed with a linear dependence on the horizon H (Osband and Van Roy 2017), because regret is accumulated once per episode through the value gap at the initial state of each episode. In contrast, our discounted infinite-horizon regret accumulates a value gap at every interaction time t . Since each value gap itself represents a discounted future loss over an effective horizon of order $(1-\gamma)^{-1}$, this per-step regret criterion introduces an additional effective-horizon factor, leading to the $(1-\gamma)^{-2}$ dependence in our bound.

The Bayesian robust regret for AQ-BRMDP, $BR-R(T)$, indicates that the adaptive quantile schedule, while becoming less robust to encourage learning of the true-environment optimal policy, does not incur large cumulative regret relative to the robust-optimal value. It grows as $\tilde{O}(\sqrt{SAT})$, and increases as $\underline{\alpha}$ approaches 0 or 1, following an order of $O\left(\sqrt{\ln \frac{1}{\min\{1-\underline{\alpha}, \underline{\alpha}\}}}\right)$. This dependence is comparable to the state-action and time dependence appearing in recent tabular online robust and distributionally robust RL guarantees. For finite-horizon robust MDPs with K episodes and horizon H , Dong et al. (2022) obtain frequentist robust-regret bounds of order $\tilde{O}(H^2S\sqrt{AK})$ for (s, a) -rectangular uncertainty sets. More recent online f -divergence distributionally robust RL results obtain \sqrt{SAK} dependence, for example $\tilde{O}(\sqrt{H^4(1+\sigma)SAK})$ for χ^2 ambiguity sets, where σ is the radius of the ambiguity set (Ghosh et al. 2026). The comparison, however, should be interpreted carefully. Existing online robust RL results typically establish frequentist robust regret bounds under a fixed but unknown environment, with the benchmark given by the optimal policy for a worst-case value over an ambiguity set. Such frequentist guarantees are stronger than Bayesian regret guarantees when the model class and benchmark coincide, since a Bayesian regret bound is the prior average of the true environment regret bound. In our setting, however, the BR-MDP formulation itself is posterior-based: epistemic uncertainty is represented by the posterior distribution, and the Bellman backup is evaluated through a posterior risk criterion. Bayesian regret is therefore the natural performance measure, in the same spirit as PSRL, where regret is commonly analyzed after averaging over the prior distribution (Osband et al. 2013, Osband and Van Roy 2017, Xu et al. 2024).

5 Experiments

We evaluate AQ-BRMDP in finite-state environments with two complementary settings: RiverSwim in Section 5.1, which requires sustained exploration toward a distant rewarding state, and risky-branch FrozenLake in Section 5.2, where exploratory shortcut actions can lead to sticky holes. Appendix EC.7.6 reports the sensitivity analysis for the schedule parameter δ in AQ-BRMDP. We also implement an extension of AQ-BRMDP to continuous-state spaces and evaluate its empirical performance in a continuous-state environment

in Appendix EC.7.

We compare AQ-BRMDP with two classes of algorithms: Continuing PSRL and fixed-quantile BRMDPs, denoted by BRMDP-0.1, BRMDP-0.3, and BRMDP-0.5, which use constant quantile levels $\alpha = 0.1, 0.3, 0.5$, respectively. Continuing PSRL uses the same pseudo-episode mechanism but samples one transition kernel from the current posterior and acts optimally in the sampled MDP. The fixed-quantile BRMDP baselines use a constant quantile level throughout learning; smaller quantiles correspond to more robust policies as discussed in Section 2. For BRMDP-based methods, posterior quantiles in Bellman backups are approximated by empirical quantiles from posterior samples; the corresponding value-iteration procedure and Monte Carlo budgets are given in Appendix EC.7.1. Unless otherwise noted, curves report empirical means over 100 independent runs with 95% confidence intervals.

5.1 Exploration-Demanding Environments

We first consider RiverSwim- n with $n \in \{6, 10\}$. The state space is $\mathcal{S}_n = \{1, \dots, n\}$, the initial state is 1, and the action space is $\mathcal{A} = \{a_L, a_R\}$. The left action a_L moves deterministically to the left neighboring state, and at state 1 the next state remains 1, i.e., $P^c(s-1 | s, a_L) = 1$ for $2 \leq s \leq n$ and $P^c(1 | 1, a_L) = 1$. The rewards satisfy $r(1, a_L, s') = 0.005$, $r(n, a_R, n) = 1$, and $r(s, a, s') = 0$ otherwise. For the right action, the true transition kernel makes sustained rightward progress difficult: at interior states $2 \leq s \leq n-1$, $P^c(s+1 | s, a_R) = 0.35$, $P^c(s | s, a_R) = 0.60$, and $P^c(s-1 | s, a_R) = 0.05$; at the left end, $P^c(2 | 1, a_R) = 0.60$ and $P^c(1 | 1, a_R) = 0.40$; at the right end, $P^c(n | n, a_R) = 0.60$ and $P^c(n-1 | n, a_R) = 0.40$. The agent maintains a Dirichlet posterior over each transition vector $P_{s,a}^c$. Thus, obtaining reward 1 requires sustained rightward exploration through the chain under stochastic transitions. The ten-state version lengthens this path and makes sustained exploration harder. A schematic of RiverSwim-6 is provided in Appendix Figure EC.3.

Results. Figure 1 reports cumulative true regret, moving-average reward trajectories, and state-occupancy heatmaps for RiverSwim-6 and RiverSwim-10. The reward trajectory at time t is the moving average $\bar{r}_t^{(w)} := w^{-1} \sum_{\tau=t-w+1}^t r_\tau$ with a window size of $w = 100$. The state-occupancy heatmap reports the empirical state-occupancy measure $\hat{d}_T(s) := T^{-1} \sum_{t=0}^{T-1} \mathbf{1}\{s_t = s\}$. In RiverSwim-10, the fixed-quantile BRMDP baselines behave similarly and their curves largely overlap in the cumulative-regret and moving-average-reward panels.

We have the following observations.

- (1) **Sustained exploration by AQ-BRMDP.** Compared with Continuing PSRL, AQ-BRMDP achieves lower cumulative regret in both RiverSwim-6 and RiverSwim-10. Its moving-average reward increases more quickly early in learning, indicating that it reaches the right end of the chain earlier. The occupancy heatmaps also show that AQ-BRMDP spends more time in states near the right end of the chain, especially in RiverSwim-10. These observations indicate that AQ-BRMDP supports more effective sustained exploration than Continuing PSRL.
- (2) **Effect of fixed quantile levels.** The fixed-quantile BRMDP baselines show that small quantile levels can be overly conservative in exploration-demanding environments. In RiverSwim-6, BRMDP-0.1 remains concentrated near state 1, its moving-average reward stays close to the local reward 0.005, and its cumulative regret is the largest among the fixed-quantile baselines. BRMDP-0.5 reaches states near the right end of the chain more often and attains higher moving-average rewards. In RiverSwim-10, all three fixed-quantile baselines remain concentrated near the initial state and their cumulative regret grows approximately linearly.

These results are consistent with the mechanism in Section EC.4. A fixed lower-tail quantile can make the policy too conservative to move away from the initial region and collect the data needed to reach the right

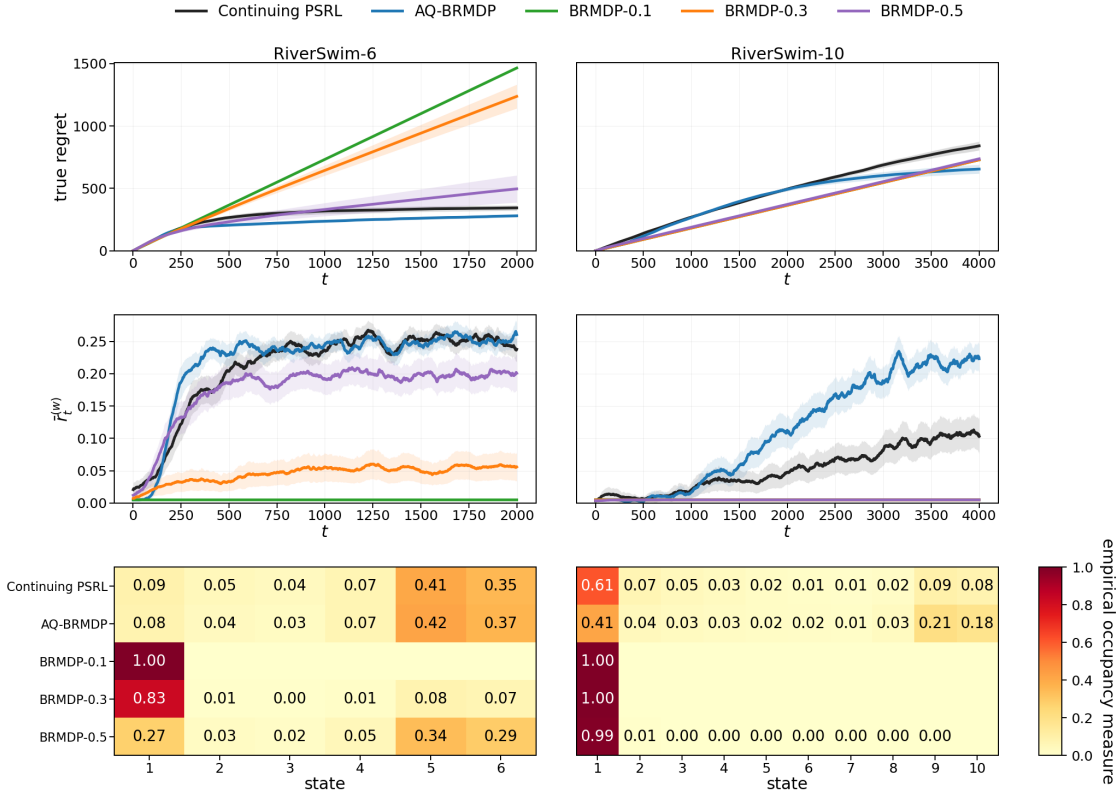


Figure 1: Performance in RiverSwim-6 (left column) and RiverSwim-10 (right column). The first row shows cumulative true regret, the second row shows moving-average rewards with a window size of 100, and the third row shows state-occupancy heatmaps.

end of the chain. By contrast, the adaptive quantile schedule in AQ-BRMDP reduces this conservatism over learning and improves exploration toward distant high-reward states.

5.2 Exploration-Costly Environments

We next consider a risky-branch variant of FrozenLake. A description of this problem is provided in Appendix Figure EC.3. The environment is a 4×4 grid with states indexed by $\mathcal{S} = \{0, \dots, 15\}$, initial state $s_0 = 0$, goal state $s_G = 15$, and hole states $H = \{5, 7, 11, 12\}$. The action space is $\mathcal{A} = \{\text{Left, Right, Up, Down}\}$. The reward is known: a transition to s_G gives reward 1, and all other transitions give reward 0. For each state that is neither a hole nor the goal, the transition is slippery. If the agent chooses an action a , then with probability 0.50 the next state follows the intended move, and with probability 0.25 for each perpendicular direction, it follows one of the two directions perpendicular to a . If a realized move leaves the grid, the agent remains in the current state. For $h \in H$ and action a , the agent moves in the intended direction with probability p_h and remains at h with probability $1 - p_h$; we set $p_h = 0.2$. After the agent reaches the goal, the next state is sampled from a uniform distribution supported on the non-hole, non-goal states. The risky shortcut is at the state-action pair (2, Down). Under the true transition kernel, taking action Down at state 2 does not follow the default slippery transition rule. Instead, $P^c(10 | 2, \text{Down}) = 1 - \theta$ and $P^c(5 | 2, \text{Down}) = \theta$. Thus, this action can shorten the path to the goal when it succeeds, but with probability θ it sends the agent into a sticky hole. We consider $\theta = 0.7$ and $\theta = 0.9$. The agent treats the entire transition kernel P^c as unknown

and maintains an independent Dirichlet posterior over each $P_{s,a}^c$.

In this environment, we also compute the posterior 0.1-quantile value defined in (12) to evaluate the robustness of the policy executed during learning. For a time step t in pseudo-episode k , let $\phi_t := \phi_k$ and $\pi_t := \pi_k$. The posterior 0.1-quantile value for the value of π_t at the initial state s_0 , $V_{\phi_t,0.1}^{\pi_t,q}(s_0)$, means that when π_t is deployed in the true environment, its value exceeds $V_{\phi_t,0.1}^{\pi_t,q}(s_0)$ with posterior probability at least 0.9. Hence, a larger $V_{\phi_t,0.1}^{\pi_t,q}(s_0)$ indicates better robustness performance under the current posterior. As discussed in Appendix EC.7.5, we estimate $V_{\phi_t,0.1}^{\pi_t,q}(s_0)$ via Monte Carlo sampling and report the approximate $\widehat{V}_{\phi_t,0.1}^{\pi_t,q}(s_0)$ in Figure 3.

Results. Figures 2 and 3 show the following patterns.

- (1) **Effective robustness–exploration trade-off.** The cumulative robust-regret and true-regret curves together show that AQ-BRMDP achieves lower regret than Continuing PSRL under both criteria. This indicates that the adaptive quantile schedule can keep the policy robust relative to the optimal value of the α -quantile BR-MDP while also effectively learning the true-optimal policy.
- (2) **Reduced true regret of BRMDP-based policies in risky environments.** In both settings, AQ-BRMDP and the BRMDP- α baselines accumulate lower true regret than Continuing PSRL. This indicates that BRMDP-based policies are more effective in those risky-shortcut environments. The reason is that when the shortcut transition is not yet well estimated, a posterior sample may underestimate $P^c(5 | 2, \text{Down})$, making policies that route the agent through state 2 appear overly favorable. Under the true kernel, however, repeated use of action Down at state 2 can move the agent to the sticky hole with high probability and produce larger regret. BRMDP-based policies instead conservatively evaluate the shortcut through posterior quantiles, and therefore tend to avoid the risky branch.
- (3) **Non-monotone effect of fixed quantile levels.** The BRMDP- α baselines reduce this early cost by evaluating lower-tail performance and therefore tend to avoid sticky holes and the risky branch. Among these baselines, BRMDP-0.3 generally yields lower regret than BRMDP-0.5, showing that some robustness is useful when the shortcut transition is not yet well estimated. However, BRMDP-0.1 can have higher regret than BRMDP-0.3, indicating that excessive conservatism may also cause large true regret. Thus, the performance of BRMDP- α is not monotone in the quantile level α .
- (4) **Posterior robustness under adaptive scheduling.** AQ-BRMDP generally attains the largest posterior 0.1-quantile value in both settings, showing that its executed policies maintain stronger posterior robustness while still improving true regret relative to Continuing PSRL.

6 Conclusions

This paper studies the α -quantile BR-MDP from both modeling and algorithmic perspectives. From a modeling perspective, we formulate the α -quantile BR-MDP, in which the quantile level provides a flexible way to adjust the risk attitude toward epistemic uncertainty. The formulation can induce robust or exploratory behavior. We further characterize this flexibility through an asymptotic normality result: for a fixed policy, the α -quantile BR-MDP value function differs from the true value function by a mean term whose sign is determined by whether α is above or below $1/2$, and whose magnitude increases as α moves farther into either tail and shrinks as the posterior concentrates. The posterior quantile value result further provides a finite-sample robustness interpretation for lower-tail quantile evaluation. From an algorithmic perspective, we develop AQ-BRMDP to account for the evolving robustness–exploration trade-off in online RL. The

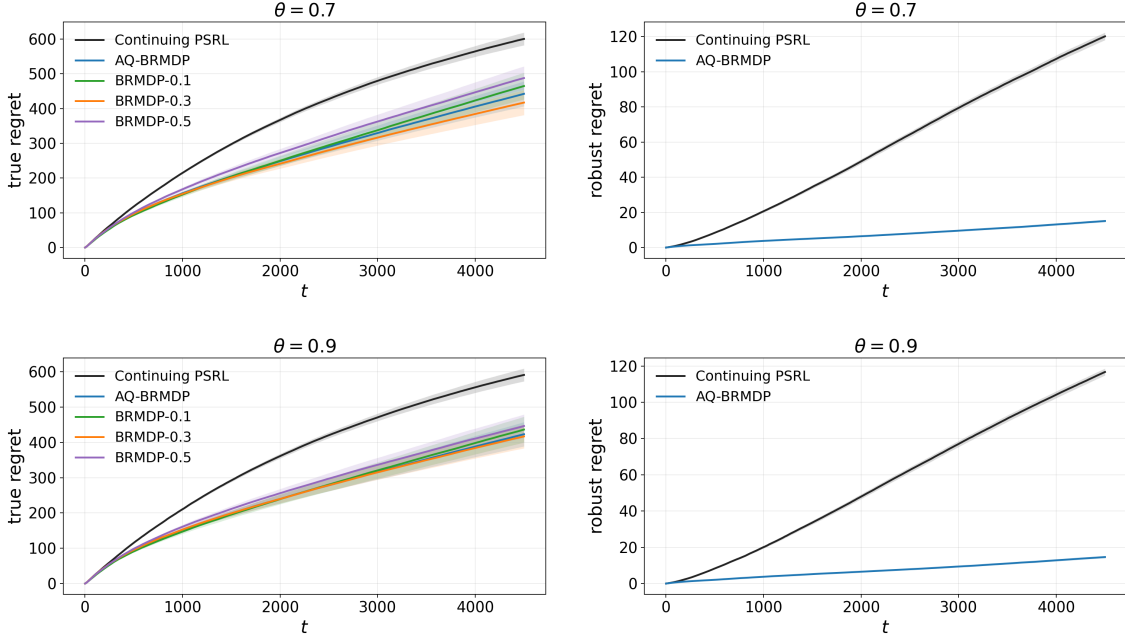


Figure 2: Cumulative true regret (left column) and cumulative robust regret with $\underline{\alpha} = 0.2$ (right column) in risky-branch FrozenLake for $\theta = 0.7$ and $\theta = 0.9$.

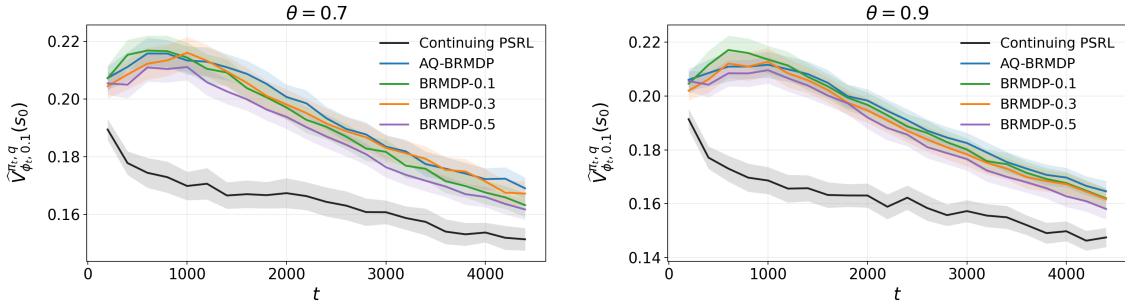


Figure 3: Posterior 0.1-quantile value $\widehat{V}_{\phi_t, 0.1}^{\pi_t, q}(s_0)$ in risky-branch FrozenLake for $\theta = 0.7$ and $\theta = 0.9$.

adaptive schedule varies with the pseudo-episode index and relative state-action visit counts, allowing the policy to be more conservative early in learning and less conservative when further exploration is needed. We theoretically prove a sublinear Bayesian regret bound and numerically demonstrate that AQ-BRMDP performs effectively in both exploration-demanding and exploration-costly environments. We also implement an extension of the proposed algorithm to continuous-state spaces and evaluate its empirical performance in a continuous-state environment.

Several directions remain open. The present analysis is developed for finite state and action spaces with direct transition parameterization and Dirichlet posteriors. Extending the formulation and the theoretical guarantees to continuous-state and continuous-action spaces would broaden the scope of the approach. On the computational side, the method relies on repeated posterior sampling and solving the quantile BR-MDP at the beginning of each pseudo-episode. Although sampling transition kernels from the Dirichlet posterior is carried out in the simulator rather than through the more costly online interaction with the true environment,

it can still materially increase computational cost. It would therefore be useful to understand how previously sampled transition kernels can be reused.

Acknowledgments

This work was supported by the Air Force Office of Scientific Research (AFOSR) under Grant FA9550-25-1-0310 and the National Science Foundation under Award ECCS-2419562.

References

- Abbasi-Yadkori Y, Szepesvári C (2015) Bayesian optimal control of smoothly parameterized systems. *Proceedings of the Thirty-First Conference on Uncertainty in Artificial Intelligence*, 1–11.
- Agrawal S, Jia R (2023) Optimistic posterior sampling for reinforcement learning: Worst-case regret bounds. *Mathematics of Operations Research* 48(1):363–392.
- Azar MG, Osband I, Munos R (2017) Minimax regret bounds for reinforcement learning. *Proceedings of the 34th International Conference on Machine Learning*, volume 70 of *Proceedings of Machine Learning Research*, 263–272.
- Badrinath KP, Kalathil D (2021) Robust reinforcement learning using least squares policy iteration with provable performance guarantees. *Proceedings of the 38th International Conference on Machine Learning*, volume 139 of *Proceedings of Machine Learning Research*, 511–520.
- Bartlett PL, Tewari A (2009) REGAL: A regularization based algorithm for reinforcement learning in weakly communicating MDPs. *Proceedings of the Twenty-Fifth Conference on Uncertainty in Artificial Intelligence*, 35–42 (AUAI Press).
- Blanchet J, Lu M, Zhang T, Zhong H (2023) Double pessimism is provably efficient for distributionally robust offline reinforcement learning: Generic algorithm and robust partial coverage. *Advances in Neural Information Processing Systems*, volume 36.
- Boucheron S, Gassiat E (2009) A Bernstein–von Mises theorem for discrete probability distributions. *Electronic Journal of Statistics* 3:114–148.
- Brafman RI, Tennenholtz M (2002) R-MAX: A general polynomial time algorithm for near-optimal reinforcement learning. *Journal of Machine Learning Research* 3:213–231.
- Delage E, Mannor S (2010) Percentile optimization for Markov decision processes with parameter uncertainty. *Operations Research* 58(1):203–213, URL <http://dx.doi.org/10.1287/opre.1080.0685>.
- Der Kiureghian A, Ditlevsen O (2009) Aleatory or epistemic? Does it matter? *Structural Safety* 31(2):105–112.
- Dong J, Li J, Wang B, Zhang J (2022) Online policy optimization for robust MDP. ArXiv:2209.13841.
- Dong K, Wang Y, Chen X, Wang L (2020) Q-learning with UCB exploration is sample efficient for infinite-horizon MDP. *International Conference on Learning Representations*.
- Duff MO (2002) *Optimal Learning: Computational Procedures for Bayes-adaptive Markov Decision Processes*. Ph.D. thesis, University of Massachusetts Amherst.
- Dulac-Arnold G, Levine N, Mankowitz DJ, Li J, Paduraru C, Gowal S, Hester T (2021) Challenges of real-world reinforcement learning: Definitions, benchmarks and analysis. *Machine Learning* 110(9):2419–2468.
- Garcelon E, Ghavamzadeh M, Lazaric A, Pirota M (2020) Conservative exploration in reinforcement learning. *Proceedings of the Twenty Third International Conference on Artificial Intelligence and Statistics*, volume 108 of *Proceedings of Machine Learning Research*, 1431–1441.
- Ghavamzadeh M, Mannor S, Pineau J, Tamar A (2015) Bayesian reinforcement learning: A survey. *Foundations and Trends in Machine Learning* 8(5–6):359–483.
- Ghosh D, Atia GK, Wang Y (2026) ORVIT: Near-optimal online distributionally robust reinforcement learning. *Proceedings of the AAAI Conference on Artificial Intelligence* 40(25):21278–21286.

- He J, Zhou D, Gu Q (2021) Nearly minimax optimal reinforcement learning for discounted MDPs. *Advances in Neural Information Processing Systems*, volume 34, 22288–22300.
- Iyengar GN (2005) Robust dynamic programming. *Mathematics of Operations Research* 30(2):257–280.
- Jaksch T, Ortner R, Auer P (2010) Near-optimal regret bounds for reinforcement learning. *Journal of Machine Learning Research* 11(51):1563–1600.
- Jin C, Allen-Zhu Z, Bubeck S, Jordan MI (2018) Is Q-learning provably efficient? *Advances in Neural Information Processing Systems*, volume 31.
- Kearns M, Singh S (2002) Near-optimal reinforcement learning in polynomial time. *Machine Learning* 49(2–3):209–232.
- Liang B, Xu L, Taneja A, Tambe M, Janson L (2025) Context in public health for underserved communities: A Bayesian approach to online restless bandits. *Proceedings of the AAAI Conference on Artificial Intelligence* 39(27):28195–28203.
- Lin Y, Ren Y, Zhou E (2022) Bayesian risk Markov decision processes. *Advances in Neural Information Processing Systems*, volume 35, 17430–17442.
- Lin Y, Zhou E (2025) Approximate bilevel difference convex programming for Bayesian risk Markov decision processes. *Proceedings of the AAAI Conference on Artificial Intelligence* 39(25):26605–26613.
- Lu M, Zhong H, Zhang T, Blanchet J (2024) Distributionally robust reinforcement learning with interactive data collection: Fundamental hardness and near-optimal algorithms. *Advances in Neural Information Processing Systems*, volume 37.
- Ma J, Lee WS (2026) EUBRL: Epistemic uncertainty directed Bayesian reinforcement learning. *International Conference on Learning Representations*.
- Nilim A, El Ghaoui L (2005) Robust control of Markov decision processes with uncertain transition matrices. *Operations Research* 53(5):780–798.
- Osband I, Russo D, Van Roy B (2013) (More) efficient reinforcement learning via posterior sampling. *Advances in Neural Information Processing Systems*, volume 26.
- Osband I, Van Roy B (2016) Posterior sampling for reinforcement learning without episodes. *arXiv preprint arXiv:1608.02731*.
- Osband I, Van Roy B (2017) Why is posterior sampling better than optimism for reinforcement learning? *Proceedings of the 34th International Conference on Machine Learning*, volume 70 of *Proceedings of Machine Learning Research*, 2701–2710 (PMLR).
- Panaganti K, Kalathil D (2022) Sample complexity of robust reinforcement learning with a generative model. *Proceedings of The 25th International Conference on Artificial Intelligence and Statistics*, volume 151 of *Proceedings of Machine Learning Research*, 9582–9602.
- Panaganti K, Xu Z, Kalathil D, Ghavamzadeh M (2022) Robust reinforcement learning using offline data. *Advances in Neural Information Processing Systems*, volume 35, 32211–32224.
- Poupart P, Vlassis N, Hoey J, Regan K (2006) An analytic solution to discrete Bayesian reinforcement learning. *Proceedings of the 23rd International Conference on Machine Learning*, 697–704.
- Puterman ML (1994) *Markov Decision Processes: Discrete Stochastic Dynamic Programming* (New York: John Wiley & Sons).
- Ross S, Chaib-draa B, Pineau J (2007) Bayes-adaptive POMDPs. *Advances in Neural Information Processing Systems*, volume 20, 1225–1232.
- Russo DJ, Van Roy B, Kazerouni A, Osband I, Wen Z (2018) A tutorial on Thompson sampling. *Foundations and Trends in Machine Learning* 11(1):1–96.
- Strehl AL, Li L, Wiewiora E, Langford J, Littman ML (2006) PAC model-free reinforcement learning. *Proceedings of the 23rd International Conference on Machine Learning*, 881–888 (ACM).
- Strehl AL, Littman ML (2008) An analysis of model-based interval estimation for Markov decision processes. *Journal of Computer and System Sciences* 74(8):1309–1331.
- Tarbouriech J, Lattimore T, O’Donoghue B (2023) Probabilistic inference in reinforcement learning done right. *ArXiv:2311.13294*.

- Tiapkin D, Belomestny D, Moulines E, Naumov A, Samsonov S, Tang Y, Valko M, Menard P (2022) From Dirichlet to Rubin: Optimistic exploration in RL without bonuses. *Proceedings of the 39th International Conference on Machine Learning*, volume 162 of *Proceedings of Machine Learning Research*, 21380–21431.
- Wang Y, Zhou E (2023) Bayesian risk-averse Q-learning with streaming observations. *Advances in Neural Information Processing Systems*, volume 36.
- Wang Y, Zhou E (2025) Online Bayesian risk-averse reinforcement learning. *arXiv preprint arXiv:2509.14077* .
- Wang Y, Zou S (2021) Online robust reinforcement learning with model uncertainty. *Advances in Neural Information Processing Systems*, volume 34, 7193–7206.
- Wiesemann W, Kuhn D, Rustem B (2013) Robust Markov decision processes. *Mathematics of Operations Research* 38(1):153–183.
- Wu D, Zhu H, Zhou E (2018) A Bayesian risk approach to data-driven stochastic optimization: Formulations and asymptotics. *SIAM Journal on Optimization* 28(2):1588–1612.
- Xu H, Mannor S (2010) Distributionally robust Markov decision processes. *Advances in Neural Information Processing Systems*, volume 23.
- Xu W, Dong S, Van Roy B (2024) Posterior sampling for continuing environments. *Reinforcement Learning Conference (RLC)*.
- Yamagata T, Santos-Rodríguez R (2024) Safe and robust reinforcement learning: Principles and practice. ArXiv:2403.18539.
- Zhou E, Xie W (2015) Simulation optimization when facing input uncertainty. *Proceedings of the 2015 Winter Simulation Conference*, 3714–3724.
- Zhou Z, Zhou Z, Bai Q, Qiu L, Blanchet J, Glynn P (2021) Finite-sample regret bound for distributionally robust offline tabular reinforcement learning. *Proceedings of The 24th International Conference on Artificial Intelligence and Statistics*, volume 130 of *Proceedings of Machine Learning Research*, 3331–3339.

Appendix: Proofs and Implementation Details

EC.1 Dirichlet Posterior Update for the Transition Kernel

Let $\Delta^{\mathcal{S}} := \{p \in \mathbb{R}_+^{\mathcal{S}} : \sum_{s' \in \mathcal{S}} p(s') = 1\}$ denote the probability simplex. For a parameter vector $\eta \in \mathbb{R}_{++}^{\mathcal{S}}$, let $\text{Dir}(\eta)$ denote the Dirichlet distribution on $\Delta^{\mathcal{S}}$ with density

$$f(p \mid \eta) \propto \prod_{s' \in \mathcal{S}} p(s')^{\eta(s')-1}.$$

For each state-action pair (s, a) , we place the prior $P_{s,a} \sim \text{Dir}(\phi_0(s, a))$, where $\phi_0(s, a) = (\phi_0(s, a, s'))_{s' \in \mathcal{S}}$ is the prior parameter vector with $\phi_0(s, a, s') > 0$. The prior parameter $\phi_0(s, a)$ can be chosen based on prior knowledge; in the absence of such information, a common choice is the uniform Dirichlet prior $\phi_0(s, a, s') = 1$ for all $s' \in \mathcal{S}$.

Let $N(s, a, s')$ be the number of observed transitions from (s, a) to s' , let $N(s, a) := \sum_{s' \in \mathcal{S}} N(s, a, s')$ denote the number of visits to (s, a) , and let $N := \sum_{s,a} N(s, a)$ denote the total number of observations. Define the σ -field generated by the observed transitions as $\mathcal{F}_N = \sigma\{(s_i, a_i, s_{i+1}) : i = 0, \dots, N-1\}$. By conjugacy, the posterior is

$$P_{s,a} \mid \mathcal{F}_N \sim \text{Dir}(\phi_N(s, a)),$$

where

$$\phi_N(s, a, s') = \phi_0(s, a, s') + N(s, a, s'), \quad \forall s' \in \mathcal{S}. \quad (\text{EC.1})$$

Thus, the posterior parameter ϕ_N is determined by the prior parameter ϕ_0 and the transition counts induced by the observed trajectory. In the main text, when the current posterior is fixed, we suppress the dependence on N and write $\phi(s, a)$ for $\phi_N(s, a)$.

EC.2 Proof of Asymptotic Normality

Lemma 4 (Basic properties of the quantile functional). *Let ρ^α be the left α -quantile functional, $\alpha \in (0, 1)$. Then for any real random variables X, Y :*

- (i) for any constant $c \in \mathbb{R}$, $\rho^\alpha(X + c) = \rho^\alpha(X) + c$;
- (ii) for any constant $c > 0$, $\rho^\alpha(cX) = c \rho^\alpha(X)$;
- (iii) if $X \geq Y$ almost surely, then $\rho^\alpha(X) \geq \rho^\alpha(Y)$;
- (iv) if $|X - Y| \leq c$ almost surely for some $c \geq 0$, then $|\rho^\alpha(X) - \rho^\alpha(Y)| \leq \|X - Y\|_\infty \leq c$.

Let $(\Omega, \mathcal{F}, \mathbb{P})$ be the underlying probability space on which the observed transition process is defined. For each N , let $\mathcal{D}_N := \{s_0, a_0, s_1, \dots, s_{N-1}, a_{N-1}, s_N\}$ be the trajectory data in Assumption 1(i), and set $\mathcal{F}_N := \sigma(\mathcal{D}_N)$. For the martingale argument below, write $\mathcal{F}_i := \sigma(s_0, a_0, \dots, s_i, a_i)$ for the history before observing s_{i+1} , $i = 0, \dots, N-1$. Throughout this proof, $O_p(\cdot)$, $o_p(\cdot)$, and \xrightarrow{P} are understood with respect to the randomness of the observed data under \mathbb{P} as $N \rightarrow \infty$.

For any integer $m \geq 2$ and any probability vector $p \in \mathbb{R}_+^m$ with $\sum_{i=1}^m p_i = 1$, define $\Sigma(p) := \text{diag}(p) - pp^\top$. Define the transition counts $N(s, a, s') := \sum_{i=0}^{N-1} \mathbb{I}\{s_i = s, a_i = a, s_{i+1} = s'\}$, and then $N(s, a) = \sum_{s' \in \mathcal{S}} N(s, a, s')$. For each (s, a) with $N(s, a) > 0$, define $\tilde{P}_N(s, a)(s') = \frac{N(s, a, s')}{N(s, a)}$. Under the uniform Dirichlet prior, the posterior parameter satisfies $\phi(s, a, s') = N(s, a, s') + 1$.

Here and below, for a real-valued posterior random variable X_N and a real-valued random variable X with cdf F , we write

$$X_N \mid \mathcal{F}_N \Rightarrow X \quad \text{in } \mathbb{P}\text{-probability}$$

to mean conditional weak convergence in probability. More precisely, for every bounded continuous test function $\psi : \mathbb{R} \rightarrow \mathbb{R}$,

$$\mathbb{E}[\psi(X_N) | \mathcal{F}_N] - \mathbb{E}[\psi(X)] \xrightarrow{\mathbb{P}} 0.$$

The conditional expectation is taken with respect to the posterior distribution given \mathcal{F}_N , whereas the convergence in probability is with respect to the randomness of the observed data.

Lemma 5 is a fixed-dimensional Dirichlet special case of the Bernstein–von Mises theorem for discrete probability distributions (Boucheron and Gassiat 2009); we restate it in the form needed here.

Lemma 5 (Posterior CLT for a Dirichlet transition vector). *For $(s, a) \in \mathcal{S} \times \mathcal{A}$, suppose $P_{s,a} | \mathcal{F}_N \sim \text{Dir}(\phi(s, a))$. Then, conditionally on \mathcal{F}_N , as $N(s, a) \rightarrow \infty$,*

$$\sqrt{N(s, a)}(P_{s,a} - \tilde{P}_N(s, a)) \Rightarrow \mathcal{N}(0, \Sigma(P_{s,a}^c))$$

in \mathbb{P} -probability.

Proof. The Bernstein–von Mises (BvM) theorem applies directly to the coordinates $J_+ := \{x : P_{s,a}^c(x) > 0\}$, on which the true transition vector lies in the relative interior of the simplex (Boucheron and Gassiat 2009). For $x \in J_0 := \{x : P_{s,a}^c(x) = 0\}$, no transition to x is observed almost surely, so $N(s, a, x) = 0$. Since the prior parameters are fixed and positive, $\mathbb{E}[P_{s,a}(x) | \mathcal{F}_N] = O(N(s, a)^{-1})$, and hence $P_{s,a}(x) = O_p(N(s, a)^{-1})$. Therefore

$$\sqrt{N(s, a)}(P_{s,a}(x) - \tilde{P}_N(s, a)(x)) = \sqrt{N(s, a)}P_{s,a}(x) \xrightarrow{p} 0.$$

Combining the BvM limit on J_+ with this degenerate limit on J_0 gives the stated Gaussian limit with covariance $\Sigma(P_{s,a}^c)$, possibly singular. \square

In the following lemma, we show that conditional weak convergence of random variables implies convergence of the corresponding conditional quantiles.

Lemma 6. *Let $(Z_N)_{N \geq 1}$ be real-valued random variables on $(\Omega, \mathcal{F}, \mathbb{P})$, and let $(\mathcal{F}_N)_{N \geq 1}$ be a sequence of sub- σ -fields of \mathcal{F} . For each N , define the conditional cdf of Z_N given \mathcal{F}_N by*

$$F_N(x) := \mathbb{P}(Z_N \leq x | \mathcal{F}_N), \quad x \in \mathbb{R},$$

Assume that there exists a real-valued random variable Z with cdf F such that $Z_N | \mathcal{F}_N \Rightarrow Z$ in \mathbb{P} -probability. For $\alpha \in (0, 1)$, define

$$q_N := \inf\{x \in \mathbb{R} : F_N(x) \geq \alpha\}, \quad q_\alpha := \inf\{x \in \mathbb{R} : F(x) \geq \alpha\}.$$

If F is continuous and strictly increasing on a neighborhood of q_α , then

$$q_N \xrightarrow{p} q_\alpha.$$

In particular, if $F = \Phi$ is the standard normal cdf, then $q_\alpha = \Phi^{-1}(\alpha) = z_\alpha$, and hence $q_N \xrightarrow{p} z_\alpha$.

Proof. Fix a continuity point x of F and $\delta > 0$. For $\varepsilon > 0$, define

$$\psi_{x,\varepsilon}^-(t) := \begin{cases} 1, & t \leq x - \varepsilon, \\ 1 - \frac{t - (x - \varepsilon)}{\varepsilon}, & x - \varepsilon < t < x, \\ 0, & t \geq x, \end{cases} \quad \psi_{x,\varepsilon}^+(t) := \begin{cases} 1, & t \leq x, \\ 1 - \frac{t - x}{\varepsilon}, & x < t < x + \varepsilon, \\ 0, & t \geq x + \varepsilon. \end{cases}$$

Then $\psi_{x,\varepsilon}^- \leq \mathbf{1}\{t \leq x\} \leq \psi_{x,\varepsilon}^+$, so

$$\mathbb{E}[\psi_{x,\varepsilon}^-(Z_N) | \mathcal{F}_N] \leq F_N(x) \leq \mathbb{E}[\psi_{x,\varepsilon}^+(Z_N) | \mathcal{F}_N].$$

By the assumed conditional weak convergence,

$$\mathbb{E}[\psi_{x,\varepsilon}^\pm(Z_N) | \mathcal{F}_N] \xrightarrow{p} \mathbb{E}[\psi_{x,\varepsilon}^\pm(Z)].$$

Since F is continuous at x , $\mathbb{E}[\psi_{x,\varepsilon}^-(Z)] \uparrow F(x)$ and $\mathbb{E}[\psi_{x,\varepsilon}^+(Z)] \downarrow F(x)$ as $\varepsilon \downarrow 0$. Choose $\varepsilon > 0$ so that

$$F(x) - \frac{\delta}{2} \leq \mathbb{E}[\psi_{x,\varepsilon}^-(Z)] \leq F(x) \leq \mathbb{E}[\psi_{x,\varepsilon}^+(Z)] \leq F(x) + \frac{\delta}{2}.$$

Then

$$\mathbb{P}(F_N(x) < F(x) - \delta) \leq \mathbb{P}\left(\mathbb{E}[\psi_{x,\varepsilon}^-(Z_N) \mid \mathcal{F}_N] < \mathbb{E}[\psi_{x,\varepsilon}^-(Z)] - \frac{\delta}{2}\right) \rightarrow 0,$$

and similarly,

$$\mathbb{P}(F_N(x) > F(x) + \delta) \leq \mathbb{P}\left(\mathbb{E}[\psi_{x,\varepsilon}^+(Z_N) \mid \mathcal{F}_N] > \mathbb{E}[\psi_{x,\varepsilon}^+(Z)] + \frac{\delta}{2}\right) \rightarrow 0.$$

Hence

$$F_N(x) \xrightarrow{P} F(x).$$

For $\varepsilon > 0$ small enough that $F(q_\alpha - \varepsilon) < \alpha < F(q_\alpha + \varepsilon)$, which is possible because F is continuous and strictly increasing on a neighborhood of q_α , we have

$$F_N(q_\alpha - \varepsilon) \xrightarrow{P} F(q_\alpha - \varepsilon), \quad F_N(q_\alpha + \varepsilon) \xrightarrow{P} F(q_\alpha + \varepsilon).$$

Hence, $\mathbb{P}(F_N(q_\alpha - \varepsilon) < \alpha < F_N(q_\alpha + \varepsilon)) \rightarrow 1$. By the definition of the left quantile, this implies $\mathbb{P}(q_\alpha - \varepsilon < q_N \leq q_\alpha + \varepsilon) \rightarrow 1$. Therefore $q_N \xrightarrow{P} q_\alpha$. \square

Lemma 7 (Posterior quantile expansion for bounded linear forms). *For $(s, a) \in \mathcal{S} \times \mathcal{A}$, suppose $N(s, a) \rightarrow \infty$. Let v_N be an \mathcal{F}_N -measurable random vector such that $\|v_N\|_\infty \leq B$ almost surely for some constant $B < \infty$ and assume that $v_N \xrightarrow{P} v$ for some deterministic vector $v \in \mathbb{R}^S$. Define $\sigma^2(s, a; v_N) := v_N^\top \Sigma(P_{s,a}^c) v_N$. Then*

$$\rho_{\phi(s,a)}^\alpha(P^\top v_N) = \tilde{P}_N(s, a)^\top v_N + \frac{z_\alpha}{\sqrt{N(s, a)}} \sigma(s, a; v_N) + o_p(N(s, a)^{-1/2}).$$

Proof. Conditionally on \mathcal{F}_N , the vector v_N is deterministic. If $\sigma(s, a; v) = 0$, then v is constant on the support of $P_{s,a}^c$, and Lemma 5 together with $v_N \xrightarrow{P} v$ implies $P^\top v_N - \tilde{P}_N(s, a)^\top v_N = o_p(N(s, a)^{-1/2})$; moreover $\sigma(s, a; v_N) \rightarrow 0$, so the variance term is also $o_p(N(s, a)^{-1/2})$. Thus it remains to consider the case $\sigma(s, a; v) > 0$.

By Lemma 5 and the continuous mapping theorem,

$$Z_N := \frac{\sqrt{N(s, a)}(P^\top v_N - \tilde{P}_N(s, a)^\top v_N)}{\sigma(s, a; v_N)} \mid \mathcal{F}_N \Rightarrow \mathcal{N}(0, 1)$$

in \mathbb{P} -probability. Let $F_N(x) := \mathbb{P}(Z_N \leq x \mid \mathcal{F}_N)$, $x \in \mathbb{R}$, denote the posterior conditional cdf of Z_N given \mathcal{F}_N . Applying Lemma 6 with $F = \Phi$, we obtain

$$\rho^\alpha(Z_N) = z_\alpha + o_p(1).$$

Now write

$$P^\top v_N = \tilde{P}_N(s, a)^\top v_N + \frac{\sigma(s, a; v_N)}{\sqrt{N(s, a)}} Z_N.$$

Using Lemma 4(i)–(ii),

$$\rho_{\phi(s,a)}^\alpha(P^\top v_N) = \tilde{P}_N(s, a)^\top v_N + \frac{\sigma(s, a; v_N)}{\sqrt{N(s, a)}} (z_\alpha + o_p(1)).$$

Finally, since $\sigma(s, a; v_N)^2 = v_N^\top \Sigma(P_{s,a}^c) v_N \leq \|v_N\|_\infty^2 \leq B^2$ almost surely, we have $\sigma(s, a; v_N) = O_p(1)$, and therefore

$$\frac{\sigma(s, a; v_N)}{\sqrt{N(s, a)}} o_p(1) = o_p(N(s, a)^{-1/2}).$$

This proves the claim. \square

Lemma 8 (Martingale CLT for empirical transition frequencies). *Under Assumption 1,*

$$\left(\sqrt{N}(\tilde{P}_N(s, \pi(s)) - P_{s, \pi(s)}^c)^\top V^\pi\right)_{s \in \mathcal{S}} \Rightarrow \mathcal{N}\left(0, \text{diag}(\sigma_\pi^2(s))_{s \in \mathcal{S}}\right),$$

where

$$\sigma_\pi^2(s) = \frac{1}{\bar{n}_s} (V^\pi)^\top \Sigma(P_{s, \pi(s)}^c) V^\pi.$$

Moreover, for each $s \in \mathcal{S}$, $\|\tilde{P}_N(s, \pi(s)) - P_{s, \pi(s)}^c\|_\infty = O_p(N(s, \pi(s))^{-1/2}) = O_p(N^{-1/2})$.

Proof. For each $s \in \mathcal{S}$, define

$$D_{i+1}^s := \mathbb{I}\{s_i = s, a_i = \pi(s)\} \left(V^\pi(s_{i+1}) - (P_{s, \pi(s)}^c)^\top V^\pi \right), \quad i = 0, \dots, N-1.$$

By Assumption 1(i), $\mathbb{E}_{s_{i+1} \sim P_{s, \pi(s)}^c} [D_{i+1}^s \mid \mathcal{F}_i] = 0$. Hence $M_N^s := \sum_{i=0}^{N-1} D_{i+1}^s$ is a sum of martingale differences. For $s, \tilde{s} \in \mathcal{S}$, the conditional covariance satisfies

$$\sum_{i=0}^{N-1} \mathbb{E}[D_{i+1}^s D_{i+1}^{\tilde{s}} \mid \mathcal{F}_i] = \mathbb{I}\{s = \tilde{s}\} N(s, \pi(s)) (V^\pi)^\top \Sigma(P_{s, \pi(s)}^c) V^\pi.$$

Indeed, if $s \neq \tilde{s}$, the two indicators cannot both be one at the same time. Dividing by N and using Assumption 1(i),

$$\frac{1}{N} \sum_{i=0}^{N-1} \mathbb{E}[D_{i+1}^s D_{i+1}^{\tilde{s}} \mid \mathcal{F}_i] \xrightarrow{\text{a.s.}} \mathbb{I}\{s = \tilde{s}\} \bar{n}_s (V^\pi)^\top \Sigma(P_{s, \pi(s)}^c) V^\pi.$$

Since the state space is finite and V^π is bounded, the increments are uniformly bounded, so the conditional Lindeberg condition holds. The multivariate martingale CLT gives

$$\left(\frac{M_N^s}{\sqrt{N}}\right)_{s \in \mathcal{S}} \Rightarrow \mathcal{N}\left(0, \text{diag}\left(\bar{n}_s (V^\pi)^\top \Sigma(P_{s, \pi(s)}^c) V^\pi\right)_{s \in \mathcal{S}}\right).$$

Finally, note that $M_N^s = N(s, \pi(s)) (\tilde{P}_N(s, \pi(s)) - P_{s, \pi(s)}^c)^\top V^\pi$. Therefore,

$$\sqrt{N}(\tilde{P}_N(s, \pi(s)) - P_{s, \pi(s)}^c)^\top V^\pi = \frac{N}{N(s, \pi(s))} \frac{M_N^s}{\sqrt{N}}.$$

Slutsky's theorem and Assumption 1(i) imply the stated joint convergence.

It remains to show the rate bound. For each $s, x \in \mathcal{S}$, define

$$D_{i+1}^{s,x} := \mathbb{I}\{s_i = s, a_i = \pi(s)\} (\mathbb{I}\{s_{i+1} = x\} - P^c(x \mid s, \pi(s))).$$

The same martingale argument gives $\sum_{i=0}^{N-1} D_{i+1}^{s,x} = O_p(N^{1/2})$. Since

$$\tilde{P}_N(s, \pi(s))(x) - P^c(x \mid s, \pi(s)) = \frac{1}{N(s, \pi(s))} \sum_{i=0}^{N-1} D_{i+1}^{s,x},$$

and $N(s, \pi(s)) \asymp N$ by Assumption 1(i), we obtain $\tilde{P}_N(s, \pi(s))(x) - P^c(x \mid s, \pi(s)) = O_p(N^{-1/2})$. The state space is finite, so the same bound holds in sup norm. \square

Next, we are ready to prove Theorem 1.

Proof of Theorem 1. Let $\Delta_N := V_{\phi, \alpha}^\pi - V^\pi$. For each state $s \in \mathcal{S}$, we define the posterior quantile map, for notational simplicity, $q_{N,s}(v) := \rho_{\phi(s, \pi(s))}^\alpha(P^\top v)$.

Recall that $V_{\phi, \alpha}^\pi$ and V^π are the unique fixed points of (5) and (3), respectively. Hence we have the two fixed-point equations:

$$V_{\phi, \alpha}^\pi(s) = r(s, \pi(s)) + \gamma q_{N,s}(V_{\phi, \alpha}^\pi), \quad V^\pi(s) = r(s, \pi(s)) + \gamma (P_{s, \pi(s)}^c)^\top V^\pi.$$

For each $s \in \mathcal{S}$,

$$\begin{aligned}\Delta_N(s) &= \gamma \left(q_{N,s}(V_{\phi,\alpha}^\pi) - (P_{s,\pi(s)}^c)^\top V^\pi \right) \\ &= \gamma \left(q_{N,s}(V^\pi) - (P_{s,\pi(s)}^c)^\top V^\pi \right) + \gamma (P_{s,\pi(s)}^c)^\top \Delta_N \\ &\quad + \gamma \left(q_{N,s}(V_{\phi,\alpha}^\pi) - q_{N,s}(V^\pi) - (P_{s,\pi(s)}^c)^\top \Delta_N \right).\end{aligned}$$

Therefore, componentwise,

$$\begin{aligned}((I - \gamma P_\pi^c) \Delta_N)(s) &= \underbrace{\gamma \left(q_{N,s}(V^\pi) - (P_{s,\pi(s)}^c)^\top V^\pi \right)}_{B_N(s)} + \underbrace{\gamma \left(q_{N,s}(V_{\phi,\alpha}^\pi) - q_{N,s}(V^\pi) - (P_{s,\pi(s)}^c)^\top \Delta_N \right)}_{R_N(s)}.\end{aligned}\tag{EC.2}$$

We next identify the weak limit of B_N . Fix $s \in \mathcal{S}$ and $a = \pi(s)$. Define $\tilde{\sigma}_\pi^2(s) := (V^\pi)^\top \Sigma(P_{s,a}^c) V^\pi$. Lemma 7 with $v_N \equiv V^\pi$ yields

$$q_{N,s}(V^\pi) = \tilde{P}_N(s, a)^\top V^\pi + \frac{z_\alpha}{\sqrt{N(s, a)}} \tilde{\sigma}_\pi(s) + o_p(N(s, a)^{-1/2}),\tag{EC.3}$$

Combining (EC.3) with Assumption 1(i),

$$\sqrt{N} \left(q_{N,s}(V^\pi) - (P_{s,\pi(s)}^c)^\top V^\pi \right) = \sqrt{N} \left(\tilde{P}_N(s, \pi(s)) - P_{s,\pi(s)}^c \right)^\top V^\pi + z_\alpha \sqrt{\frac{N}{N(s, \pi(s))}} \tilde{\sigma}_\pi(s) + o_p(1).$$

By Lemma 8, the first term on the right-hand side converges jointly to a centered normal vector. Since $N(s, \pi(s))/N \xrightarrow{\text{a.s.}} \bar{n}_s$, Slutsky's theorem gives

$$\left(\sqrt{N} \left(q_{N,s}(V^\pi) - (P_{s,\pi(s)}^c)^\top V^\pi \right) \right)_{s \in \mathcal{S}} \Rightarrow \mathcal{N} \left(\lambda_\pi, \text{diag}(\sigma_\pi^2(s))_{s \in \mathcal{S}} \right),$$

where

$$\sigma_\pi^2(s) = \frac{(\tilde{\sigma}_\pi(s))^2}{\bar{n}_s} = \frac{1}{\bar{n}_s} (V^\pi)^\top \left(\text{diag}(P_{s,\pi(s)}^c) - P_{s,\pi(s)}^c (P_{s,\pi(s)}^c)^\top \right) V^\pi, \quad \lambda_\pi(s) := z_\alpha \sigma_\pi(s).$$

Therefore,

$$\sqrt{N} B_N \Rightarrow \mathcal{N} \left(\gamma \lambda_\pi, \text{diag}((\gamma \sigma_\pi)^2) \right).\tag{EC.4}$$

We now derive the rate of Δ_N itself. From the fixed-point equations (5) and (3),

$$\Delta_N(s) = \gamma \left(q_{N,s}(V_{\phi,\alpha}^\pi) - q_{N,s}(V^\pi) \right) + B_N(s).$$

Taking sup norms and using Lemma 4(iv), $\|\Delta_N\|_\infty \leq \gamma \|\Delta_N\|_\infty + \|B_N\|_\infty$. Hence $\|\Delta_N\|_\infty \leq \frac{1}{1-\gamma} \|B_N\|_\infty$. Since (EC.4) implies $\sqrt{N} B_N$ is tight,

$$\|\Delta_N\|_\infty = O_p(N^{-1/2}).\tag{EC.5}$$

It remains to show that the remainder R_N is negligible. Fix again $s \in \mathcal{S}$ and set $a = \pi(s)$. Define, for any $v \in \mathbb{R}^S$, $\sigma^2(s, a; v) := v^\top \Sigma(P_{s,a}^c) v$. By (EC.5), $V_{\phi,\alpha}^\pi \xrightarrow{p} V^\pi$, so the convergence condition in Lemma 7 is satisfied. Applying Lemma 7 twice, first with $v_N = V_{\phi,\alpha}^\pi$, then with $v_N \equiv V^\pi$, we have

$$\begin{aligned}q_{N,s}(V_{\phi,\alpha}^\pi) - q_{N,s}(V^\pi) &= \tilde{P}_N(s, a)^\top \Delta_N \\ &\quad + \frac{z_\alpha}{\sqrt{N(s, a)}} \left(\sigma(s, a; V_{\phi,\alpha}^\pi) - \sigma(s, a; V^\pi) \right) + o_p(N(s, a)^{-1/2}).\end{aligned}\tag{EC.6}$$

Substituting (EC.6) into (EC.2),

$$\begin{aligned}R_N(s) &= \gamma \left(\tilde{P}_N(s, a) - P_{s,a}^c \right)^\top \Delta_N \\ &\quad + \frac{\gamma z_\alpha}{\sqrt{N(s, a)}} \left(\sigma(s, a; V_{\phi,\alpha}^\pi) - \sigma(s, a; V^\pi) \right) + o_p(N(s, a)^{-1/2}).\end{aligned}\tag{EC.7}$$

We estimate the middle term in (EC.7). Let $A^c(s, a) := \Sigma(P_{s,a}^c)$. Since $A^c(s, a)$ is positive semidefinite, $\sigma(s, a; v) = \|A^c(s, a)^{1/2}v\|_2$. Hence,

$$\begin{aligned} & \left| \sigma(s, a; V_{\phi, \alpha}^\pi) - \sigma(s, a; V^\pi) \right| \\ &= \left| \|A^c(s, a)^{1/2}V_{\phi, \alpha}^\pi\|_2 - \|A^c(s, a)^{1/2}V^\pi\|_2 \right| \\ &\leq \|A^c(s, a)^{1/2}(V_{\phi, \alpha}^\pi - V^\pi)\|_2 \leq \|A^c(s, a)^{1/2}\|_{\text{op}} \|\Delta_N\|_2. \end{aligned}$$

Since $A^c(s, a) \preceq \text{diag}(P_{s,a}^c) \preceq I$, $\|A^c(s, a)\|_{\text{op}}^{1/2} \leq 1$. Therefore

$$\left| \sigma(s, a; V_{\phi, \alpha}^\pi) - \sigma(s, a; V^\pi) \right| \leq \|A^c(s, a)\|_{\text{op}}^{1/2} \|\Delta_N\|_2 \leq \sqrt{S} \|\Delta_N\|_\infty = O_p(N^{-1/2}).$$

After division by $\sqrt{N(s, a)}$, the middle term in (EC.7) becomes $O_p(N^{-1})$.

For the first term in (EC.7), Lemma 8 gives

$$\|\tilde{P}_N(s, a) - P_{s,a}^c\|_\infty = O_p(N(s, a)^{-1/2}) = O_p(N^{-1/2}),$$

while (EC.5) gives $\|\Delta_N\|_\infty = O_p(N^{-1/2})$. Hence

$$(\tilde{P}_N(s, a) - P_{s,a}^c)^\top \Delta_N = O_p(N^{-1}).$$

Since also $o_p(N(s, a)^{-1/2}) = o_p(N^{-1/2})$, we conclude from (EC.7) that $R_N(s) = o_p(N^{-1/2})$, $\forall s \in \mathcal{S}$. Because $S < \infty$,

$$\sqrt{N} R_N \xrightarrow{p} 0. \quad (\text{EC.8})$$

Finally, multiply (EC.2) by \sqrt{N} :

$$\sqrt{N} (I - \gamma P_\pi^c) \Delta_N = \sqrt{N} B_N + \sqrt{N} R_N.$$

By (EC.4), (EC.8), and Slutsky's theorem,

$$\sqrt{N} (I - \gamma P_\pi^c) (V_{\phi, \alpha}^\pi - V^\pi) \Rightarrow \mathcal{N}(\gamma \lambda_\pi, \text{diag}((\gamma \sigma_\pi)^2)).$$

Since P_π^c is row-stochastic, $\|\gamma P_\pi^c\|_\infty \leq \gamma < 1$, so $(I - \gamma P_\pi^c)^{-1}$ exists and is bounded. Applying the continuous mapping theorem to the linear map $(I - \gamma P_\pi^c)^{-1}$ yields

$$\sqrt{N} (V_{\phi, \alpha}^\pi - V^\pi) \Rightarrow \mathcal{N}\left((I - \gamma P_\pi^c)^{-1} \gamma \lambda_\pi, (I - \gamma P_\pi^c)^{-1} \text{diag}((\gamma \sigma_\pi)^2) (I - \gamma P_\pi^c)^{-T}\right).$$

This completes the proof. \square

EC.3 Proof of Proposition 1

Proof. Fix a policy π . By the definition of the left $\bar{\alpha}$ -quantile, for each $s \in \mathcal{S}$,

$$\mathbb{P}_\phi \left(P_{s, \pi(s)}^\top V_{\phi, \bar{\alpha}}^\pi \geq \rho_{\phi(s, \pi(s))}^{\bar{\alpha}} (P^\top V_{\phi, \bar{\alpha}}^\pi) \right) \geq 1 - \bar{\alpha}.$$

Using the Bellman equation for $V_{\phi, \bar{\alpha}}^\pi$, this implies

$$\mathbb{P}_\phi \left(r(s, \pi(s)) + \gamma P_{s, \pi(s)}^\top V_{\phi, \bar{\alpha}}^\pi \geq V_{\phi, \bar{\alpha}}^\pi(s) \right) \geq 1 - \bar{\alpha}.$$

Because the posterior rows $(P_{s, \pi(s)})_{s \in \mathcal{S}}$ are independent across states under \mathbb{P}_ϕ , the above events are independent. Hence,

$$\mathbb{P}_\phi \left(r(s, \pi(s)) + \gamma P_{s, \pi(s)}^\top V_{\phi, \bar{\alpha}}^\pi \geq V_{\phi, \bar{\alpha}}^\pi(s), \quad \forall s \in \mathcal{S} \right) \geq (1 - \bar{\alpha})^S = 1 - \alpha.$$

On this event,

$$V_{\phi, \bar{\alpha}}^\pi(s) \leq r(s, \pi(s)) + \gamma P_{s, \pi(s)}^\top V_{\phi, \bar{\alpha}}^\pi, \quad \forall s \in \mathcal{S}.$$

Let \mathcal{T}_P^π denote the standard Bellman operator under policy π and realized transition matrix P :

$$(\mathcal{T}_P^\pi V)(s) := r(s, \pi(s)) + \gamma P_{s, \pi(s)}^\top V, \quad \forall s \in \mathcal{S}.$$

The preceding event implies $V_{\phi, \bar{\alpha}}^\pi \leq \mathcal{T}_P^\pi V_{\phi, \bar{\alpha}}^\pi$ componentwise. By monotonicity of \mathcal{T}_P^π , $V_{\phi, \bar{\alpha}}^\pi \leq (\mathcal{T}_P^\pi)^m V_{\phi, \bar{\alpha}}^\pi$, $\forall m \geq 1$. Since \mathcal{T}_P^π is a γ -contraction under $\|\cdot\|_\infty$, its iterates converge to the unique fixed point V_P^π . Letting $m \rightarrow \infty$ yields $V_{\phi, \bar{\alpha}}^\pi \leq V_P^\pi$ componentwise on the above event. Then the claim follows immediately from the definition of $V_{\phi, \alpha}^{\pi, q}(s)$ in (12). \square

EC.4 Evolving Robustness–Exploration Trade-off in Online RL: Illustrative Examples

In online RL, the balance between robustness and exploration evolves over the course of learning. When the posterior distribution is still dispersed and epistemic uncertainty is relatively large across all state–action pairs, robustness induced by lower-tail evaluation (lower quantile level) can be beneficial. As more data are collected, the remaining epistemic uncertainty about $P_{s,a}^c$ becomes concentrated in less-visited state–action pairs, which remain critical for learning the optimal policy in the true environment. In this regime, a higher quantile level encourages exploration of these state–action pairs that have higher epistemic uncertainty. The examples in this subsection separately illustrate these two mechanisms and show why a fixed lower-tail rule, i.e., choosing actions according to the optimal policy of the α -quantile BR-MDP with a fixed α , fails to learn the optimal policy.

We begin with a regime in which the balance tilts toward robustness. For any transition kernel P , let V_P^* denote the optimal value function under P . Given a posterior distribution φ over transition kernels, let $\bar{P}_\varphi := \mathbb{E}_{P \sim \varphi}[P]$ denote the posterior-mean kernel. We denote by $\pi_{\varphi, \alpha}^*$ an optimal risk-aware policy of the α -quantile BR-MDP under the posterior φ , and by $\pi_{\bar{P}_\varphi}^*$ an optimal risk-neutral policy under the posterior-mean kernel \bar{P}_φ . The latter is obtained by replacing P^c with \bar{P}_φ in (4) and solving the resulting Bellman optimality equation. To make precise when robustness is needed in this regime, we introduce the notion of posterior downside exposure in the following definition.

Definition 1 (Posterior downside exposure). Fix a posterior distribution φ over transition kernels, an initial state s_0 , a policy π , and a threshold $\Lambda > 0$. Define the set of transition kernels under which the regret of policy π is at least the threshold Λ as follows:

$$\mathcal{D}(\pi, \Lambda) := \left\{ P : V_P^*(s_0) - V_P^\pi(s_0) \geq \Lambda \right\}.$$

We say that π has (β, Λ) -posterior downside exposure under φ if $\varphi(\mathcal{D}(\pi, \Lambda)) \geq \beta$.

Definition 1 measures how much posterior mass is placed on transition kernels under which the regret of policy π is at least Λ from the initial state s_0 .

Example 1 (A posterior downside-exposure example). Fix a discount factor $\gamma \in (0, 1)$, a constant $c \in (0, \gamma)$, and a loss level $L > 0$. Consider the discounted MDP in Figure EC.1, where the reward is known to the agent but the transition kernel is unknown. The current posterior is supported on two kernels,

$$\varphi = \mu \delta_{PG} + (1 - \mu) \delta_{PB}, \quad \mu \in (0, 1),$$

where δ_x denotes the Dirac measure at x , and PG and PB differ only in the transition following the risky action a_R at the initial state s_0 , as shown in the figure.

Proposition 2. In Example 1, if $\frac{\gamma(1-L)}{2} < c < \gamma(\mu - (1 - \mu)L)$, $\mu > 1/2$, and $\alpha \leq 1 - \mu$, then $\pi_{\bar{P}_\varphi}^*(s_0) = a_R$ and $\pi_{\varphi, \alpha}^*(s_0) = a_S$. Moreover, for every Λ satisfying $\frac{\gamma-c}{1-\gamma} < \Lambda \leq \frac{c+\gamma L}{1-\gamma}$, the optimal policy under the

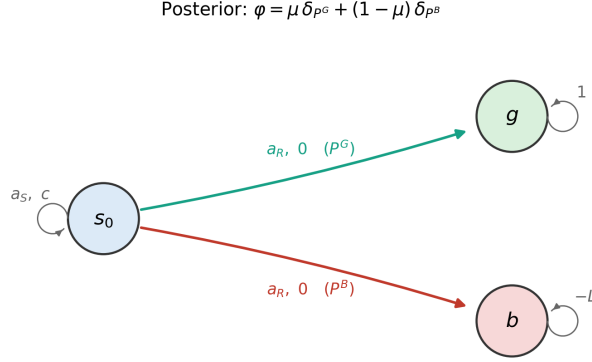


Figure EC.1: Schematic of Example 1. From the initial state s_0 , the safe action a_S yields reward c and returns to s_0 . The risky action a_R yields reward 0. Under P^G , it moves to the absorbing state g , which yields reward 1 at every subsequent step; under P^B , it moves to the absorbing state b , which yields reward $-L$ at every subsequent step.

posterior-mean kernel $\pi_{\bar{P}\varphi}^*$ has $(1 - \mu, \Lambda)$ -posterior downside exposure, whereas the regret of $\pi_{\varphi, \alpha}^*$ is below the threshold Λ with posterior probability one, i.e.,

$$\varphi\left(\mathcal{D}_\varphi(\pi_{\bar{P}\varphi}^*, \Lambda)\right) = 1 - \mu, \quad \varphi\left(\mathcal{D}_\varphi(\pi_{\varphi, \alpha}^*, \Lambda)\right) = 0.$$

The proof of Proposition 2 is deferred to Appendix EC.4.1. The proposition highlights a failure mode of posterior-mean planning under model uncertainty. Since the posterior-mean kernel averages over the possible transition models, it assigns a higher posterior-mean value to a_R than to a_S ; However, this averaged comparison hides the fact that, with posterior probability $1 - \mu$, the selected action a_R leads to the bad absorbing state b and receives reward $-L$ thereafter. Under those posterior models, the posterior-mean policy suffers regret above the threshold Λ specified in Proposition 2. In contrast, when $\alpha \leq 1 - \mu$, the α -quantile BR-MDP is sensitive to this lower-tail posterior outcome: it penalizes a_R for its performance on the models where a_R leads to b , and therefore selects the safe action a_S .

We next consider a regime in which the balance shifts toward exploration. An action can matter because after observing the transition it generates, the posterior distribution can become substantially more concentrated, or even collapse to a point mass at the true transition kernel. This becomes important once the main issue is no longer the large posterior downside exposure defined in Definition 1 but whether taking the action substantially reduces the remaining epistemic uncertainty that matters for subsequent decisions. The next example illustrates this situation by contrasting an explorative action, whose transition reveals the kernel, with a safe action that leaves the posterior unchanged. Let $\varphi^{(s, a, s')}$ denote the updated posterior distribution after observing (s, a, s') .

Example 2 (An informative exploration example). Fix a discount factor $\gamma \in (0, 1)$ and a constant $c \in (0, \gamma)$. Consider the discounted MDP in Figure EC.2, where the reward is known to the agent but the transition kernel is unknown. The current posterior is supported on two kernels,

$$\varphi = \mu \delta_{P^G} + (1 - \mu) \delta_{P^B}, \quad \mu \in (0, 1),$$

where P^G and P^B differ only along the branch reached after taking the explorative action shown in the figure.

This example isolates a situation in which an action is valuable because of the information it reveals: after taking a_E at s_0 , the next-state observation reveals the kernel, so $\varphi^{(s_0, a_E, y_G)} = \delta_{P^G}$, and $\varphi^{(s_0, a_E, y_B)} = \delta_{P^B}$. The optimal subsequent action can then be selected according to the updated posterior: take a_X at y_G and a_S at y_B . Therefore, taking a_E at s_0 produces an observation that fully resolves the remaining uncertainty

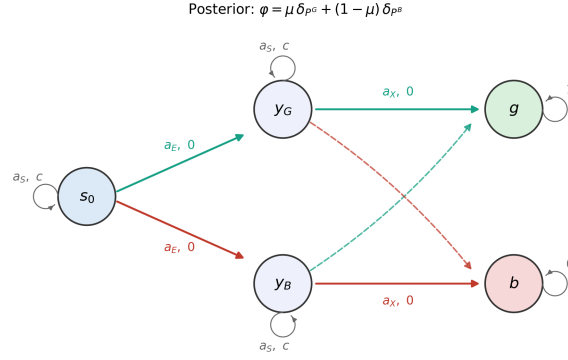


Figure EC.2: Schematic of Example 2. From the initial state s_0 , the safe action a_S yields reward c and returns to s_0 , whereas the exploratory action a_E yields reward 0 and moves to y_G under P^G and to y_B under P^B . At each diagnostic state $y \in \{y_G, y_B\}$, action a_S yields reward c and stays at y , whereas action a_X yields reward 0 and moves to the absorbing state g under P^G and to the absorbing state b under P^B . State g yields reward 1 at every subsequent step, and state b yields reward 0 at every subsequent step. All other transitions are identical under P^G and P^B . Hence, the transition observed after (s_0, a_E) reveals the kernel, whereas (s_0, a_S) reveals no new information.

relevant to subsequent decisions. By contrast, taking the safe action a_S at s_0 does not change the posterior: $P^G(s_0|s_0, a_S) = P^B(s_0|s_0, a_S) = 1$, so observing (s_0, a_S, s_0) cannot provide additional information for distinguishing P^G from P^B , and hence $\varphi^{(s_0, a_S, s_0)} = \varphi$.

The next proposition shows that a fixed lower-tail rule can nevertheless avoid this informative action indefinitely. Once the agent chooses a_S , the posterior never changes, so the same decision rule continues to choose a_S at every subsequent visit to s_0 . If the true kernel is P^G , this yields linear regret.

Proposition 3. *In Example 2, assume that $\alpha \leq 1 - \mu$ and $c < \gamma^2$. Suppose that after each realized transition the agent updates its posterior and then acts according to an optimal policy of the α -quantile BR-MDP, $\pi_t := \pi_{\varphi_t, \alpha}^*$ at time step t . If the initial state is s_0 and the prior distribution $\varphi_0 = \varphi$, then*

$$\varphi_t = \varphi, \quad a_t = \pi_t(s_t) = a_S \quad \text{and} \quad s_{t+1} = s_0 \quad \forall t \geq 0.$$

If the true kernel is P^G , then under the cumulative regret criterion $R_T := \sum_{t=0}^{T-1} (V_{P^G}^(s_t) - V_{P^G}^{\pi_t}(s_t))$, one has $R_T = T \frac{\gamma^2 - c}{1 - \gamma}$.*

The proof of Proposition 3 is deferred to Appendix EC.4.2. It shows how a fixed lower-tail rule can create what we call a self-confirming trap: under the current posterior, the optimal policy of the α -quantile BR-MDP is suboptimal in the true environment, yet following this policy generates no new information to update the posterior. As a result, re-solving the same α -quantile BR-MDP under the unchanged posterior and fixed quantile level α selects the same action again. When the true kernel is P^G , the fixed lower-tail rule continues to choose a_S and the agent therefore never discovers the higher future value available after probing, which leads to linear regret.

Taken together, these results show that the robustness induced by the lower-tail quantile can be desirable when posterior downside exposure is substantial due to high epistemic uncertainty, but that using a fixed lower-tail rule can later hinder informative exploration and create a self-confirming trap with linear regret. The reason is that the trade-off between robustness and exploration evolves over learning.

EC.4.1 Proof of Proposition 2

Proof. Let $R_{\bar{P}} := \frac{\gamma(\mu - (1 - \mu)L)}{1 - \gamma}$. Under the posterior-mean kernel \bar{P}_φ , if action a_R is taken at s_0 , the value obtained after the transition is $R_{\bar{P}} = \mu \frac{\gamma}{1 - \gamma} + (1 - \mu) \frac{-\gamma L}{1 - \gamma}$. The optimal value at s_0 under \bar{P}_φ satisfies

$$V_{\bar{P}_\varphi}^*(s_0) = \max \left\{ c + \gamma V_{\bar{P}_\varphi}^*(s_0), R_{\bar{P}} \right\}.$$

Since $\gamma(\mu - (1 - \mu)L) > c$, we have $R_{\bar{P}} > \frac{c}{1 - \gamma}$. Equivalently, $c + \gamma R_{\bar{P}} < R_{\bar{P}}$. Hence the fixed point is $V_{\bar{P}_\varphi}^*(s_0) = R_{\bar{P}}$, and the unique optimal action at s_0 is a_R . Therefore $\pi_{\bar{P}_\varphi}^*(s_0) = a_R$.

Next consider the lower-tail α -quantile BR-MDP. Since g and b are absorbing, $V(g) = \frac{1}{1 - \gamma}$, and $V(b) = \frac{-L}{1 - \gamma}$. Under a_R , the posterior distribution of the next-state value is $\frac{1}{1 - \gamma}$ with probability μ , $\frac{-L}{1 - \gamma}$ with probability $1 - \mu$. Since $\alpha \leq 1 - \mu$, the left α -quantile is $\frac{-L}{1 - \gamma}$. Thus the BRMDP value of taking a_R at s_0 is $R_\alpha := -\frac{\gamma L}{1 - \gamma}$. The BRMDP optimal value at s_0 therefore satisfies

$$V_{\varphi, \alpha}^*(s_0) = \max \left\{ c + \gamma V_{\varphi, \alpha}^*(s_0), R_\alpha \right\}.$$

Because $c > 0$ and $L > 0$, $\frac{c}{1 - \gamma} > -\frac{\gamma L}{1 - \gamma} = R_\alpha$. Hence the fixed point is $V_{\varphi, \alpha}^*(s_0) = \frac{c}{1 - \gamma}$, and the optimal action is a_S . Therefore $\pi_{\varphi, \alpha}^*(s_0) = a_S$.

We now compute the regret under each realized kernel. Since $c < \gamma(\mu - (1 - \mu)L) \leq \gamma$, under P^G , taking a_R is optimal. Hence $V_{P^G}^*(s_0) = \frac{\gamma}{1 - \gamma}$. The posterior-mean policy chooses a_R , so its regret under P^G is zero. The BRMDP policy chooses a_S , so

$$V_{P^G}^*(s_0) - V_{P^G}^{\pi_{\varphi, \alpha}^*}(s_0) = \frac{\gamma}{1 - \gamma} - \frac{c}{1 - \gamma} = \frac{\gamma - c}{1 - \gamma}.$$

Under P^B , taking a_S is optimal because $c > 0$ and $L > 0$. Hence $V_{P^B}^*(s_0) = \frac{c}{1 - \gamma}$. The BRMDP policy chooses a_S , so its regret under P^B is zero. The posterior-mean policy chooses a_R , so

$$V_{P^B}^*(s_0) - V_{P^B}^{\pi_{\bar{P}_\varphi}^*}(s_0) = \frac{c}{1 - \gamma} - \left(-\frac{\gamma L}{1 - \gamma} \right) = \frac{c + \gamma L}{1 - \gamma}.$$

Finally, the condition $c > \frac{\gamma(1 - L)}{2}$ is equivalent to $\frac{\gamma - c}{1 - \gamma} < \frac{c + \gamma L}{1 - \gamma}$, so the stated interval for Λ is nonempty. For any $\frac{\gamma - c}{1 - \gamma} < \Lambda \leq \frac{c + \gamma L}{1 - \gamma}$, the posterior-mean policy has regret at least Λ exactly under P^B , whose posterior probability is $1 - \mu$. Therefore $\varphi\left(\mathcal{D}(\pi_{\bar{P}_\varphi}^*, \Lambda)\right) = 1 - \mu$.

On the other hand, the BRMDP policy has regret $\frac{\gamma - c}{1 - \gamma} < \Lambda$ under P^G , and regret 0 under P^B . Hence its regret is below Λ with posterior probability one, and $\varphi\left(\mathcal{D}(\pi_{\varphi, \alpha}^*, \Lambda)\right) = 0$. \square

EC.4.2 Proof of Proposition 3

Proof. Under the α -quantile BR-MDP criterion with $\alpha \leq 1 - \mu$, taking a_X at either diagnostic state yields next-state value $1/(1 - \gamma)$ with posterior mass μ and 0 with posterior mass $1 - \mu$. Therefore its left α -quantile is 0, whereas repeatedly taking the safe self-loop yields value $c/(1 - \gamma)$. Hence

$$V_{\varphi, \alpha}^*(y_G) = V_{\varphi, \alpha}^*(y_B) = \frac{c}{1 - \gamma},$$

so taking a_E at s_0 yields value $\gamma c/(1 - \gamma)$. By contrast, repeatedly taking the safe self-loop at s_0 yields value $c/(1 - \gamma)$, and delaying a_E by $k \geq 1$ safe steps yields

$$\frac{c(1 - \gamma^k) + \gamma^{k+1}c}{1 - \gamma} < \frac{c}{1 - \gamma}.$$

Thus $\pi_{\varphi, \alpha}^*(s_0) = a_S$.

Now suppose that after each realized transition the agent updates its posterior and then chooses $\pi_t := \pi_{\varphi_t, \alpha}$. Taking a_S at s_0 always produces the observation (s_0, a_S, s_0) , whose likelihood is identical under P^G and P^B . Hence Bayes updating leaves the posterior unchanged. Starting from $S_0 = s_0$ and $\varphi_0 = \varphi$, an induction gives $\varphi_t = \varphi$ and $\pi_t(s_0) = a_S$ for all $t \geq 0$; since a_S returns to s_0 , we also have $S_t = s_0$ for all t . In particular, the agent never probes.

Under P^G , taking a_E at s_0 and then a_X at y_G yields value $\gamma^2/(1-\gamma)$, whereas repeatedly taking the safe self-loop yields value $c/(1-\gamma)$. Since $c < \gamma^2$, probing strictly dominates staying safe, and delaying a_E by $k \geq 1$ safe steps yields $\frac{c(1-\gamma^k)+\gamma^{k+2}}{1-\gamma} < \frac{\gamma^2}{1-\gamma}$. Hence $V_{P^G}^*(s_0) = \gamma^2/(1-\gamma)$. On the other hand, each π_t chooses a_S at s_0 , so $V_{P^G}^{\pi_t}(s_0) = c/(1-\gamma)$. Because $S_t = s_0$ for all t , each summand in R_T equals $(\gamma^2 - c)/(1-\gamma)$, and therefore $R_T = T \frac{\gamma^2 - c}{1-\gamma}$. \square

EC.5 Value Iteration for α_k -quantile BR-MDP

At the beginning of pseudo-episode k , after computing the posterior parameter collection ϕ_k and the adaptive quantile schedule α_k , we solve the corresponding BR-MDP by value iteration.

Algorithm EC.1 Value Iteration for the α_k -quantile BR-MDP in Pseudo-Episode k

- 1: **Input:** Posterior parameter collection ϕ_k , quantile schedule α_k , optimal value function in pseudo-episode $k-1$ V_{k-1} , tolerance ε_{VI} , maximum iterations M_{VI}
 - 2: Initialize $V^{(0)} \leftarrow V_{k-1}$
 - 3: **for** $m = 0, 1, \dots, M_{\text{VI}} - 1$ **do**
 - 4: **for all** $s \in \mathcal{S}$ **do**
 - 5:
$$V^{(m+1)}(s) \leftarrow \max_{a \in \mathcal{A}} \left\{ r(s, a) + \gamma \rho_{\phi_k(s, a)}^{\alpha_k} \left(P^\top V^{(m)} \right) \right\}.$$
 - 6: **end for**
 - 7: **if** $\|V^{(m+1)} - V^{(m)}\|_\infty \leq \varepsilon_{\text{VI}}$ **then**
 - 8: **break**
 - 9: **end if**
 - 10: **end for**
 - 11: Set $V_k \leftarrow V^{(m+1)}$
 - 12: For each $s \in \mathcal{S}$, choose $\pi_k(s) \in \arg \max_{a \in \mathcal{A}} \left\{ r(s, a) + \gamma \rho_{\phi_k(s, a)}^{\alpha_k} (P^\top V_k) \right\}$
 - 13: **return** V_k, π_k
-

EC.6 Proofs of Regret Analysis

For a fixed interaction horizon T , the last pseudo-episode may be truncated. In the proof, with a slight abuse of notation, let L_k denote the full geometric length of pseudo-episode k . Equivalently, if the last pseudo-episode is truncated by the fixed horizon, we continue it only for the purpose of the proof under the same policy π_{K_T} . Since the added regret summands are nonnegative, this no-truncation convention provides an upper bound on the actual regret. Thus,

$$BR(T) \leq \mathbb{E} \left[\sum_{k=1}^{K_T} \sum_{i=1}^{L_k} \left(V^*(s_{k,i}) - V^{\pi_k}(s_{k,i}) \right) \right]. \quad (\text{EC.9})$$

It remains to bound the right-hand side under this convention.

EC.6.1 Proof of Lemma 1

Proof. From the Bayesian perspective,

$$P_{s,a}^c \mid \mathcal{F}_{t_k} \sim \text{Dir}(\phi_k(s, a)), \quad \forall (s, a) \in \mathcal{S} \times \mathcal{A},$$

where $\phi_k(s, a) = (\phi_k(s, a, s'))_{s' \in \mathcal{S}}$ denotes the Dirichlet parameter vector. For each $(s, a) \in \mathcal{S} \times \mathcal{A}$, define the event $\mathcal{G}_k(s, a) := \left\{ (P_{s,a}^c)^\top V_k \leq \rho_{\phi_k(s,a)}^{\alpha_k} (P^\top V_k) \right\}$. By the definition of the α -quantile,

$$\mathbb{P}(\mathcal{G}_k(s, a) \mid \mathcal{F}_{t_k}) = \mathbb{P}\left((P_{s,a}^c)^\top V_k \leq \rho_{\phi_k(s,a)}^{\alpha_k} (P^\top V_k) \mid \mathcal{F}_{t_k} \right) \geq \alpha_k(s, a).$$

Let $\mathcal{G}_k := \bigcap_{(s,a) \in \mathcal{S} \times \mathcal{A}} \mathcal{G}_k(s, a)$. Then

$$\begin{aligned} \mathbb{P}(\mathcal{G}_k \mid \mathcal{F}_{t_k}) &\geq 1 - \sum_{(s,a) \in \mathcal{S} \times \mathcal{A}} \mathbb{P}(\mathcal{G}_k^c(s, a) \mid \mathcal{F}_{t_k}) \geq 1 - \sum_{(s,a) \in \mathcal{S} \times \mathcal{A}} (1 - \alpha_k(s, a)) \\ &\geq 1 - \delta \frac{\ln(2k)}{\sqrt{k}} \sum_{(s,a) \in \mathcal{S} \times \mathcal{A}} \frac{N_k^+(s, a)}{\bar{N}_k^+} = 1 - \frac{\delta SA \ln(2k)}{\sqrt{k}}, \end{aligned}$$

where the third line follows from (14) and the last equality uses $\bar{N}_k^+ = \frac{1}{SA} \sum_{(s,a) \in \mathcal{S} \times \mathcal{A}} N_k^+(s, a)$.

It remains to show that on the event \mathcal{G}_k we have $V^* \leq V_k$ pointwise. Define

$$Q^*(s, a) := r(s, a) + \gamma (P_{s,a}^c)^\top V^*, \quad Q_k(s, a) := r(s, a) + \gamma \rho_{\phi_k(s,a)}^{\alpha_k} (P^\top V_k),$$

so that $V^*(s) = \max_{a \in \mathcal{A}} Q^*(s, a)$ and $V_k(s) = \max_{a \in \mathcal{A}} Q_k(s, a)$. Let $\Delta(s) := V^*(s) - V_k(s)$ and $\Delta_{\max} := \max_{s \in \mathcal{S}} \Delta(s)$. For each $s \in \mathcal{S}$, choose $a_s^* \in \arg \max_{a \in \mathcal{A}} Q^*(s, a)$. Then

$$\begin{aligned} \Delta(s) &= V^*(s) - V_k(s) \leq Q^*(s, a_s^*) - Q_k(s, a_s^*) \\ &= \gamma \left((P_{s,a_s^*}^c)^\top V^* - \rho_{\phi_k(s,a_s^*)}^{\alpha_k} (P^\top V_k) \right) \\ &= \gamma \left((P_{s,a_s^*}^c)^\top (V^* - V_k) + (P_{s,a_s^*}^c)^\top V_k - \rho_{\phi_k(s,a_s^*)}^{\alpha_k} (P^\top V_k) \right) \\ &\leq \gamma \Delta_{\max}, \end{aligned}$$

where the last inequality uses $(P_{s,a_s^*}^c)^\top (V^* - V_k) \leq \Delta_{\max}$ and, on the event \mathcal{G}_k , $(P_{s,a_s^*}^c)^\top V_k - \rho_{\phi_k(s,a_s^*)}^{\alpha_k} (P^\top V_k) \leq 0$. Hence $\Delta_{\max} \leq \gamma \Delta_{\max}$, which implies $\Delta(s) \leq \Delta_{\max} \leq 0$. That is, $V^*(s) \leq V_k(s)$ for all $s \in \mathcal{S}$ on the event \mathcal{G}_k . Combining this implication with $\mathbb{P}(\mathcal{G}_k \mid \mathcal{F}_{t_k}) \geq 1 - \frac{\delta SA \ln(2k)}{\sqrt{k}}$ proves part (i).

For part (ii), let $V^- := V_{\phi_k, \underline{\alpha}}^*$. Since $\alpha_k(s, a) \geq \underline{\alpha}$ for all $(s, a) \in \mathcal{S} \times \mathcal{A}$ and the α -quantile is nondecreasing in α , we have

$$(\mathcal{T}_{\phi_k, \underline{\alpha}}^* V)(s) \leq (\mathcal{T}_{\phi_k, \alpha_k}^* V)(s), \quad \forall V, \forall s \in \mathcal{S}.$$

Therefore,

$$V^- = \mathcal{T}_{\phi_k, \underline{\alpha}}^* V^- \leq \mathcal{T}_{\phi_k, \alpha_k}^* V^- \leq (\mathcal{T}_{\phi_k, \alpha_k}^*)^n V^-, \quad \forall n \geq 1,$$

where the last inequality follows from the monotonicity of $\mathcal{T}_{\phi_k, \alpha_k}^*$. Since $\mathcal{T}_{\phi_k, \alpha_k}^*$ is a γ -contraction, its iterates converge to its unique fixed point V_k . Letting $n \rightarrow \infty$ yields $V^- \leq V_k$, that is, $V_{\phi_k, \underline{\alpha}}^*(s) \leq V_k(s)$ for all $s \in \mathcal{S}$. This completes the proof. \square

EC.6.2 Proof of Lemma 2

Proof. Define $\Delta(s) := V_{\phi_k, \alpha_k}^\pi(s) - V^\pi(s)$ and $\Delta_{k,i} := \Delta(s_{k,i})$. By the Bellman equations for V_{ϕ_k, α_k}^π and V^π , for each $i \geq 1$,

$$\begin{aligned} \Delta_{k,i} &= \left[r(s_{k,i}, a_{k,i}) + \gamma \rho_{\phi_k(s_{k,i}, a_{k,i})}^{\alpha_k} (P^\top V_{\phi_k, \alpha_k}^\pi) \right] - \left[r(s_{k,i}, a_{k,i}) + \gamma (P_{s_{k,i}, a_{k,i}}^c)^\top V^\pi \right] \\ &= \gamma E_{k,i} + \gamma (P_{s_{k,i}, a_{k,i}}^c)^\top (V_{\phi_k, \alpha_k}^\pi - V^\pi). \end{aligned}$$

Since

$$\mathbb{E}[\Delta_{k,i+1} \mid s_{k,i}, a_{k,i}, \mathcal{F}_{t_k}, P^c] = (P_{s_{k,i}, a_{k,i}}^c)^\top \Delta,$$

the tower property gives

$$\mathbb{E}[\Delta_{k,i} \mid \mathcal{F}_{t_k}, P^c] = \gamma \mathbb{E}[E_{k,i} \mid \mathcal{F}_{t_k}, P^c] + \gamma \mathbb{E}[\Delta_{k,i+1} \mid \mathcal{F}_{t_k}, P^c]. \quad (\text{EC.10})$$

Because rewards are bounded in $[0, 1]$, both V_{ϕ_k, α_k}^π and V^π are bounded by $(1 - \gamma)^{-1}$ in sup norm. Hence $|\Delta_{k,i}| \leq \frac{1}{1-\gamma}$ and $|E_{k,i}| \leq \frac{1}{1-\gamma}$ for all $i \geq 1$. Iterating (EC.10) for $n \geq 1$ yields

$$\mathbb{E}[\Delta_{k,i} \mid \mathcal{F}_{t_k}, P^c] = \sum_{h=0}^{n-1} \gamma^{h+1} \mathbb{E}[E_{k,i+h} \mid \mathcal{F}_{t_k}, P^c] + \gamma^n \mathbb{E}[\Delta_{k,i+n} \mid \mathcal{F}_{t_k}, P^c].$$

The last term converges to zero as $n \rightarrow \infty$ because $\gamma \in (0, 1)$ and $\Delta_{k,i+n}$ is uniformly bounded. Therefore,

$$\mathbb{E}[\Delta_{k,i} \mid \mathcal{F}_{t_k}, P^c] = \sum_{h=0}^{\infty} \gamma^{h+1} \mathbb{E}[E_{k,i+h} \mid \mathcal{F}_{t_k}, P^c]. \quad (\text{EC.11})$$

Next use the pseudo-episode construction. Conditional on (\mathcal{F}_{t_k}, P^c) , the random length L_k is independent of the MDP trajectory and satisfies $\mathbb{P}(L_k \geq i \mid \mathcal{F}_{t_k}, P^c) = \gamma^{i-1}$, $i \geq 1$, because L_k is geometric with success probability $1 - \gamma$ on $\{1, 2, \dots\}$. Since $|\Delta_{k,i}| \leq (1 - \gamma)^{-1}$, we have $\mathbb{E}[\sum_{i \geq 1} \mathbf{1}\{L_k \geq i\} |\Delta_{k,i}| \mid \mathcal{F}_{t_k}, P^c] \leq (1 - \gamma)^{-2} < \infty$. Hence Fubini's theorem and conditional independence give

$$\mathbb{E}\left[\sum_{i=1}^{L_k} \Delta_{k,i} \mid \mathcal{F}_{t_k}, P^c\right] = \sum_{i=1}^{\infty} \mathbb{E}[\mathbf{1}\{L_k \geq i\} \Delta_{k,i} \mid \mathcal{F}_{t_k}, P^c] = \sum_{i=1}^{\infty} \gamma^{i-1} \mathbb{E}[\Delta_{k,i} \mid \mathcal{F}_{t_k}, P^c]. \quad (\text{EC.12})$$

Substituting (EC.11) into (EC.12) and exchanging the order of summation, which is justified by absolute summability, gives

$$\mathbb{E}\left[\sum_{i=1}^{L_k} \Delta_{k,i} \mid \mathcal{F}_{t_k}, P^c\right] = \sum_{i=1}^{\infty} \gamma^{i-1} \sum_{h=0}^{\infty} \gamma^{h+1} \mathbb{E}[E_{k,i+h} \mid \mathcal{F}_{t_k}, P^c] = \sum_{t=1}^{\infty} t \gamma^t \mathbb{E}[E_{k,t} \mid \mathcal{F}_{t_k}, P^c]. \quad (\text{EC.13})$$

Similarly, $\mathbb{E}[\sum_{t \geq 1} \mathbf{1}\{L_k \geq t\} \gamma^t |E_{k,t}| \mid \mathcal{F}_{t_k}, P^c] < \infty$, so Fubini's theorem and conditional independence give

$$\mathbb{E}\left[\sum_{t=1}^{L_k} t \gamma E_{k,t} \mid \mathcal{F}_{t_k}, P^c\right] = \sum_{t=1}^{\infty} t \gamma \mathbb{E}[\mathbf{1}\{L_k \geq t\} E_{k,t} \mid \mathcal{F}_{t_k}, P^c] = \sum_{t=1}^{\infty} t \gamma^t \mathbb{E}[E_{k,t} \mid \mathcal{F}_{t_k}, P^c]. \quad (\text{EC.14})$$

Comparing (EC.13) and (EC.14) proves (19). \square

EC.6.3 Proof of Lemma 3

Proof. Apply Lemma 2 with the risk profile α_k . This gives

$$\mathbb{E}\left[\sum_{i=1}^{L_k} \left(V_{\phi_k, \alpha_k}^\pi(s_{k,i}) - V^\pi(s_{k,i})\right) \mid \mathcal{F}_{t_k}, P^c\right] = \mathbb{E}\left[\sum_{i=1}^{L_k} i \gamma E_{k,i} \mid \mathcal{F}_{t_k}, P^c\right]. \quad (\text{EC.15})$$

Next, repeat the same argument as in Lemma 2 for the constant risk level $\underline{\alpha}$. The corresponding one-step discrepancy is

$$\rho_{\phi_k(s_{k,i}, a_{k,i})}^{\underline{\alpha}} (P^\top V_{\phi_k, \underline{\alpha}}^\pi) - (P_{s_{k,i}, a_{k,i}}^c)^\top V_{\phi_k, \underline{\alpha}}^\pi = -E_{k,i}^-.$$

Therefore,

$$\mathbb{E}\left[\sum_{i=1}^{L_k} \left(V_{\phi_k, \underline{\alpha}}^\pi(s_{k,i}) - V^\pi(s_{k,i})\right) \mid \mathcal{F}_{t_k}, P^c\right] = \mathbb{E}\left[\sum_{i=1}^{L_k} i \gamma (-E_{k,i}^-) \mid \mathcal{F}_{t_k}, P^c\right]. \quad (\text{EC.16})$$

Subtracting (EC.16) from (EC.15) and using linearity of conditional expectation, we obtain

$$\mathbb{E}\left[\sum_{i=1}^{L_k} \left(V_{\phi_k, \alpha_k}^\pi(s_{k,i}) - V_{\phi_k, \underline{\alpha}}^\pi(s_{k,i})\right) \mid \mathcal{F}_{t_k}, P^c\right] = \mathbb{E}\left[\sum_{i=1}^{L_k} i \gamma (E_{k,i} + E_{k,i}^-) \mid \mathcal{F}_{t_k}, P^c\right],$$

which is exactly (20). \square

EC.6.4 Proof of Theorem 3

Lemma 9 (Dirichlet posterior quantile deviation for BR-MDP). *Fix pseudo-episode k and $(s, a) \in \mathcal{S} \times \mathcal{A}$. Conditional on \mathcal{F}_{t_k} , let $P \sim \text{Dir}(\phi_k(s, a))$, where $\phi_k(s, a) = (\phi_k(s, a, s'))_{s' \in \mathcal{S}}$ is the Dirichlet parameter vector. Let $\phi_{k,0}(s, a) := \sum_{s' \in \mathcal{S}} \phi_k(s, a, s') = N_k(s, a) + S$ denote the scalar total concentration parameter. Define the posterior mean $\bar{P}_k(\cdot | s, a) := \phi_k(s, a) / \phi_{k,0}(s, a)$. Then for any \mathcal{F}_{t_k} -measurable vector $V \in \left[0, \frac{1}{1-\gamma}\right]^S$ and any $\alpha \in (0, 1)$,*

$$\rho_{\phi_k(s,a)}^\alpha(P^\top V) - \bar{P}_k(\cdot | s, a)^\top V \leq \frac{1}{1-\gamma} \sqrt{\frac{2}{\phi_{k,0}(s,a)} \ln\left(\frac{1}{1-\alpha}\right)}, \quad (\text{EC.17})$$

$$\bar{P}_k(\cdot | s, a)^\top V - \rho_{\phi_k(s,a)}^\alpha(P^\top V) \leq \frac{1}{1-\gamma} \sqrt{\frac{2}{\phi_{k,0}(s,a)} \ln\left(\frac{1}{\alpha}\right)}. \quad (\text{EC.18})$$

Proof. If V is constant, then $P^\top V = \bar{P}_k(\cdot | s, a)^\top V$ almost surely, and both (EC.17)–(EC.18) are trivial. Hence we only consider the non-constant case.

If $S = 1$, then $p \equiv \bar{P}_k(\cdot | s, a) \equiv 1$, so the result is again trivial. Thus it remains to consider the case $S \geq 2$. In this case, $\phi_{k,0}(s, a) = N_k(s, a) + S \geq S \geq 2$. Define $Y := (1-\gamma)P^\top V$ and $\mu := (1-\gamma)\bar{P}_k(\cdot | s, a)^\top V$. By Agrawal and Jia (2023, Lemma B.1, Lemma B.4 and the proof of Corollary B.2), we have the one-sided Gaussian tail bounds

$$\mathbb{P}(Y - \mu \geq t | \mathcal{F}_{t_k}) \leq \exp\left(-\frac{\phi_{k,0}(s, a)t^2}{2}\right),$$

$$\mathbb{P}(\mu - Y \geq t | \mathcal{F}_{t_k}) \leq \exp\left(-\frac{\phi_{k,0}(s, a)t^2}{2}\right),$$

for all $t > 0$. Taking $t = (1-\gamma)\epsilon$ in these bounds yields, for every $\epsilon > 0$,

$$\mathbb{P}(P^\top V - \bar{P}_k(\cdot | s, a)^\top V \geq \epsilon | \mathcal{F}_{t_k}) \leq \exp\left(-\frac{\phi_{k,0}(s, a)(1-\gamma)^2\epsilon^2}{2}\right), \quad (\text{EC.19})$$

$$\mathbb{P}(\bar{P}_k(\cdot | s, a)^\top V - P^\top V \geq \epsilon | \mathcal{F}_{t_k}) \leq \exp\left(-\frac{\phi_{k,0}(s, a)(1-\gamma)^2\epsilon^2}{2}\right). \quad (\text{EC.20})$$

We now prove (EC.17). Let $\epsilon_+ := \frac{1}{1-\gamma} \sqrt{\frac{2}{\phi_{k,0}(s, a)} \ln\left(\frac{1}{1-\alpha}\right)}$. Then by (EC.19),

$$\mathbb{P}(P^\top V \leq \bar{P}_k(\cdot | s, a)^\top V + \epsilon_+ | \mathcal{F}_{t_k}) \geq \alpha.$$

By the definition of the left α -quantile,

$$\rho_{\phi_k(s,a)}^\alpha(P^\top V) \leq \bar{P}_k(\cdot | s, a)^\top V + \epsilon_+,$$

which proves (EC.17).

Next, let $\epsilon_- := \frac{1}{1-\gamma} \sqrt{\frac{2}{\phi_{k,0}(s, a)} \ln\left(\frac{1}{\alpha}\right)}$. Since V is non-constant and the Dirichlet parameter vector has strictly positive components, $\phi_k(s, a, s') \geq 1$ for all $s' \in \mathcal{S}$, $P^\top V$ has a continuous distribution with a strictly increasing CDF on its support. By (EC.20),

$$\mathbb{P}(P^\top V \leq \bar{P}_k(\cdot | s, a)^\top V - \epsilon_- | \mathcal{F}_{t_k}) \leq \alpha.$$

Therefore, the preceding bound and the continuity and strict monotonicity of the CDF imply

$$\rho_{\phi_k(s,a)}^\alpha(P^\top V) \geq \bar{P}_k(\cdot | s, a)^\top V - \epsilon_-,$$

which proves (EC.18). \square

Lemma 10. Let $\gamma \in (0, 1)$ and let L_1, \dots, L_K be i.i.d. geometric random variables on $\{1, 2, \dots\}$ with $\mathbb{P}(L_k = \ell) = (1 - \gamma)\gamma^{\ell-1}$. Define $u := \max\left\{e, \frac{K}{(1-\gamma)^2}\right\}$, $m := \left\lceil \frac{1}{1-\gamma} (\log u + \log \log u + 2) \right\rceil$, and

$$\mathfrak{I} := \frac{4\gamma}{1-\gamma} (\log u + \log \log u + 4)^2.$$

Then

$$\mathbb{E} \left[\frac{1}{1-\gamma} \sum_{k=1}^K \sum_{i=1}^{L_k} i \gamma \mathbb{I}\{L_k > m\} \right] \leq \mathfrak{I}.$$

Proof. Let $q := 1 - \gamma$, and let $L \sim \text{Geom}(q)$ on $\{1, 2, \dots\}$. By linearity of expectation,

$$\mathbb{E} \left[\frac{1}{1-\gamma} \sum_{k=1}^K \sum_{i=1}^{L_k} \gamma i \mathbb{I}\{L_k > m\} \right] = \frac{K\gamma}{q} \mathbb{E} \left[\frac{L(L+1)}{2} \mathbb{I}\{L > m\} \right] \leq \frac{K\gamma}{q} \mathbb{E} [L^2 \mathbb{I}\{L > m\}].$$

By the memoryless property of the geometric distribution, conditional on $\{L > m\}$ we can write $L = m + \tilde{L}$, where $\tilde{L} \sim \text{Geom}(q)$. Hence

$$\mathbb{E} [L^2 \mathbb{I}\{L > m\}] = \gamma^m \mathbb{E} [(m + \tilde{L})^2] \leq \gamma^m \left(m^2 + \frac{2m}{q} + \frac{2}{q^2} \right).$$

Since $\gamma \leq e^{-q}$, $qm \geq \log u + \log \log u + 2$, and $K/q^2 \leq u$, we have $\gamma^m \leq e^{-2}/(u \log u)$. Also $qm \leq \log u + \log \log u + 3$. Therefore,

$$\frac{K\gamma}{q} \mathbb{E} [L^2 \mathbb{I}\{L > m\}] \leq \frac{\gamma e^{-2}}{q \log u} [(\log u + \log \log u + 3)^2 + 2(\log u + \log \log u + 3) + 2] \leq \mathfrak{I}.$$

This proves the claim. \square

With a slight abuse of notation, for each time t , let $N_t(s, a)$ denote the number of visits to (s, a) before time t .

Theorem 3. Fix a deterministic interaction horizon T . Let $u_T := \max\left\{e, \frac{T}{(1-\gamma)^2}\right\}$, $m_T := \left\lceil \frac{1}{1-\gamma} (\log u_T + \log \log u_T + 2) \right\rceil$, $\mathfrak{I}_T := \frac{4\gamma}{1-\gamma} (\log u_T + \log \log u_T + 4)^2$, and $\bar{T} := T + m_T$. Define $M_T := \frac{2(S+1)(\bar{T}+SA)\sqrt{\bar{T}}}{SA\delta \ln 2}$. Then:

1.

$$\begin{aligned} BR(T) &\leq \frac{\gamma m_T}{1-\gamma} \left(\sqrt{16 SA \bar{T} \ln \frac{1}{1-\underline{\alpha}}} + \sqrt{16 SA (\bar{T} + S^2 A) \left(\ln \left(1 + \frac{SA M_T}{\bar{T} + S^2 A} \right) + 2 \right)} \right) \\ &\quad + \sqrt{16 SA \bar{T} \ln(2SA T^3 m_T)} + \frac{\gamma SA}{1-\gamma} m_T^2 \lceil \log_2 m_T \rceil \\ &\quad + \frac{\pi^2}{6(1-\gamma)} + \mathfrak{I}_T + \frac{2\delta SA \sqrt{\bar{T}} \ln(2T)}{(1-\gamma)^2}. \end{aligned} \tag{EC.21}$$

2.

$$\begin{aligned} BR-R(T) &\leq \frac{\gamma m_T}{1-\gamma} \left(\sqrt{16 SA \bar{T} \ln \frac{1}{1-\underline{\alpha}}} + \sqrt{16 SA (\bar{T} + S^2 A) \left(\ln \left(1 + \frac{SA M_T}{\bar{T} + S^2 A} \right) + 2 \right)} \right) \\ &\quad + \sqrt{16 SA \bar{T} \ln \frac{1}{\underline{\alpha}}} + 2\sqrt{16 SA \bar{T} \ln(2SA T^3 m_T)} \\ &\quad + \frac{2\gamma SA}{1-\gamma} m_T^2 \lceil \log_2 m_T \rceil + \frac{\pi^2}{3(1-\gamma)} + 2\mathfrak{I}_T. \end{aligned} \tag{EC.22}$$

Proof. For notational convenience, extend the Bernoulli restart process and the corresponding trajectory beyond time T only for the purpose of the proof. Let $I_k^T := \mathbb{I}\{k \leq K_T\}$. Since every pseudo-episode has length at least one, $K_T \leq T$, and sums over pseudo-episodes started by time T can be written as sums over $k = 1, \dots, T$ multiplied by I_k^T .

Using the upper bound in (EC.9),

$$BR(T) \leq \mathbb{E} \left[\sum_{k=1}^T I_k^T \sum_{i=1}^{L_k} \left(V^*(s_{k,i}) - V^{\pi_k}(s_{k,i}) \right) \right].$$

Under the same no-truncation convention for the robust-optimal benchmark,

$$BR-R(T) \leq \mathbb{E} \left[\sum_{k=1}^T I_k^T \sum_{i=1}^{L_k} \left(V_{\phi_k, \underline{\alpha}}^*(s_{k,i}) - V_{\phi_k, \underline{\alpha}}^{\pi_k}(s_{k,i}) \right) \right].$$

For each started pseudo-episode k , recall $\mathcal{G}_k = \bigcap_{s,a} \mathcal{G}_k(s, a)$ is the optimism event from Lemma 1. Since $1 - \alpha_k(s, a) \leq \delta \frac{N_k^+(s, a)}{\bar{N}_k^+} \frac{\ln(2k)}{\sqrt{k}}$, we have

$$\mathbb{P}(\mathcal{G}_k^c \mid \mathcal{F}_{t_k}) \leq \sum_{s,a} (1 - \alpha_k(s, a)) \leq \delta \frac{\ln(2k)}{\sqrt{k}} \sum_{s,a} \frac{N_k^+(s, a)}{\bar{N}_k^+} = \delta SA \frac{\ln(2k)}{\sqrt{k}}.$$

Moreover, on \mathcal{G}_k , $V^*(s) \leq V_k(s) = V_{\phi_k, \alpha_k}^*(s)$, $\forall s \in \mathcal{S}$.

For part (i), define $\Delta_{k,i} := V_k(s_{k,i}) - V^{\pi_k}(s_{k,i})$. Then, for $s_{k,i}$,

$$V^*(s_{k,i}) - V^{\pi_k}(s_{k,i}) = \Delta_{k,i} + \left(V^*(s_{k,i}) - V_k(s_{k,i}) \right) \leq \Delta_{k,i} + \frac{1}{1-\gamma} \mathbb{I}\{\mathcal{G}_k^c\}.$$

Therefore,

$$BR(T) \leq \mathbb{E} \left[\sum_{k=1}^T I_k^T \sum_{i=1}^{L_k} \Delta_{k,i} \right] + \frac{1}{1-\gamma} \sum_{k=1}^T \mathbb{E} \left[I_k^T L_k \mathbb{I}\{\mathcal{G}_k^c\} \right].$$

For the non-optimistic-event term, we first use $I_k^T \leq 1$. The event \mathcal{G}_k^c is determined by (\mathcal{F}_{t_k}, P^c) , whereas the pseudo-episode length L_k is generated by the independent restart randomness within pseudo-episode k . Hence L_k is independent of \mathcal{G}_k^c and satisfies $\mathbb{E}[L_k] = 1/(1-\gamma)$. Thus,

$$\begin{aligned} \frac{1}{1-\gamma} \sum_{k=1}^T \mathbb{E} \left[I_k^T L_k \mathbb{I}\{\mathcal{G}_k^c\} \right] &\leq \frac{1}{1-\gamma} \sum_{k=1}^T \mathbb{E} \left[L_k \mathbb{I}\{\mathcal{G}_k^c\} \right] = \frac{1}{(1-\gamma)^2} \sum_{k=1}^T \mathbb{P}(\mathcal{G}_k^c) = \frac{1}{(1-\gamma)^2} \sum_{k=1}^T \mathbb{E} \left[\mathbb{P}(\mathcal{G}_k^c \mid \mathcal{F}_{t_k}) \right] \\ &\leq \frac{\delta SA}{(1-\gamma)^2} \sum_{k=1}^T \frac{\ln(2k)}{\sqrt{k}} \leq \frac{2\delta SA \sqrt{T} \ln(2T)}{(1-\gamma)^2}. \end{aligned}$$

We now bound $\mathbb{E} \left[\sum_{k=1}^T I_k^T \sum_{i=1}^{L_k} \Delta_{k,i} \right]$. For each started pseudo-episode k , define \mathcal{P}_k^1 as the event that, for all $(s, a) \in \mathcal{S} \times \mathcal{A}$,

$$\left| (\bar{P}_k(\cdot \mid s, a) - P_{s,a}^c)^\top V_k \right| \leq \frac{1}{1-\gamma} \sqrt{\frac{2 \ln(2SAT m_T t_k^2)}{N_{t_k}(s, a) + S}}.$$

Conditioned on \mathcal{F}_{t_k} , the vector V_k is deterministic and $P_{s,a}^c \mid \mathcal{F}_{t_k} \sim \text{Dir}(\phi_k(s, a))$. Hence, by (EC.19), (EC.20), and a union bound,

$$\mathbb{P}((\mathcal{P}_k^1)^c \mid \mathcal{F}_{t_k}) \leq \frac{1}{T m_T t_k^2}.$$

Using $\Delta_{k,i} \leq (1-\gamma)^{-1}$, we split according to \mathcal{P}_k^1 :

$$\mathbb{E} \left[\sum_{k=1}^T I_k^T \sum_{i=1}^{L_k} \Delta_{k,i} \right] \leq \mathbb{E} \left[\sum_{k=1}^T I_k^T \sum_{i=1}^{L_k} \Delta_{k,i} \mathbb{I}\{\mathcal{P}_k^1\} \right] + \frac{1}{1-\gamma} \sum_{k=1}^T \mathbb{E} \left[I_k^T L_k \mathbb{I}\{(\mathcal{P}_k^1)^c\} \right].$$

Since $\mathcal{P}_k^1 \in \mathcal{F}_{t_k} \vee \sigma(P^c)$, Lemma 2 gives

$$\mathbb{E} \left[\sum_{k=1}^T I_k^T \sum_{i=1}^{L_k} \Delta_{k,i} \mathbb{I}\{\mathcal{P}_k^1\} \right] = \mathbb{E} \left[\sum_{k=1}^T I_k^T \sum_{i=1}^{L_k} i \gamma E_{k,i} \mathbb{I}\{\mathcal{P}_k^1\} \right],$$

where $E_{k,i} := \rho_{\phi_k(s_{k,i}, a_{k,i})}^{\alpha_k} (P^\top V_k) - (P_{s_{k,i}, a_{k,i}}^c)^\top V_k$. Moreover, by the same independence between L_k and $\mathbb{I}\{\mathcal{P}_k^1\}^c$, and since $t_k \geq k$ and $m_T \geq (1-\gamma)^{-1}$,

$$\frac{1}{1-\gamma} \sum_{k=1}^T \mathbb{E} [I_k^T L_k \mathbb{I}\{(\mathcal{P}_k^1)^c\}] \leq \frac{\pi^2}{6(1-\gamma)}.$$

Let $N'_t(s, a) := N_t(s, a) + S$, and define

$$\mathcal{B}_k := \left\{ N'_{t_{k+1}-1}(s, a) + 1 \leq 2N'_{t_k}(s, a) \text{ for all } (s, a) \in \mathcal{S} \times \mathcal{A} \right\}.$$

For the last started pseudo-episode, t_{K_T+1} is interpreted in the proof-only continuation. Since $E_{k,i} \leq (1-\gamma)^{-1}$, the preceding Bellman-error sum is bounded by

$$\begin{aligned} & \underbrace{\frac{1}{1-\gamma} \sum_{k=1}^T I_k^T \sum_{i=1}^{L_k} \gamma i \mathbb{I}\{L_k > m_T\}}_{(I)} + \underbrace{\frac{1}{1-\gamma} \sum_{k=1}^T I_k^T \sum_{i=1}^{L_k} \gamma i \mathbb{I}\{L_k \leq m_T\} \mathbb{I}\{\mathcal{B}_k^c\}}_{(II)} \\ & + \underbrace{\sum_{k=1}^T I_k^T \sum_{i=1}^{L_k} \gamma i E_{k,i} \mathbb{I}\{L_k \leq m_T\} \mathbb{I}\{\mathcal{B}_k\} \mathbb{I}\{\mathcal{P}_k^1\}}_{(III)}. \end{aligned}$$

By Lemma 10 with $K = T$, $\mathbb{E}[(I)] \leq \mathfrak{L}_T$. For term (II), the witness-pair argument gives

$$\sum_{k=1}^T I_k^T \mathbb{I}\{L_k \leq m_T\} \mathbb{I}\{\mathcal{B}_k^c\} \leq SA \lceil \log_2 m_T \rceil,$$

and hence $\mathbb{E}[(II)] \leq \frac{\gamma SA}{1-\gamma} m_T^2 \lceil \log_2 m_T \rceil$.

It remains to bound (III). On $\{L_k \leq m_T\} \cap \mathcal{B}_k \cap \mathcal{P}_k^1$, we have $i \leq m_T$. By Lemma 9, the definition of \mathcal{P}_k^1 , and

$$\ln \frac{1}{1-\alpha_k(s, a)} \leq \ln \frac{1}{1-\underline{\alpha}} + \left(\ln \frac{\bar{N}_k^+ \sqrt{k}}{\delta N_k^+(s, a) \ln(2k)} \right)_+,$$

where $(x)_+ := \max\{x, 0\}$, we have

$$E_{k,i} \leq \frac{1}{1-\gamma} \sqrt{\frac{2 \ln \frac{1}{1-\underline{\alpha}}}{N_{t_k}(s_{k,i}, a_{k,i}) + S}} + \frac{1}{1-\gamma} \sqrt{\frac{2 \left(\ln \frac{\bar{N}_k^+ \sqrt{k}}{\delta N_k^+(s_{k,i}, a_{k,i}) \ln(2k)} \right)_+}{\sqrt{N_{t_k}(s_{k,i}, a_{k,i}) + S}}} + \frac{1}{1-\gamma} \sqrt{\frac{2 \ln(2SAT m_T t_k^2)}{N_{t_k}(s_{k,i}, a_{k,i}) + S}}.$$

Since $k \leq T$, $t_k \leq T$, $\bar{N}_k^+ \leq (\bar{T} + SA)/SA$, $\ln(2k) \geq \ln 2$, and $N_k^+(s, a) \geq (N_k(s, a) + S)/(S+1)$,

$$\left(\ln \frac{\bar{N}_k^+ \sqrt{k}}{\delta N_k^+(s, a) \ln(2k)} \right)_+ \leq \left(\ln \frac{(S+1)(\bar{T} + SA) \sqrt{\bar{T}}}{SA \delta \ln 2 (N_k(s, a) + S)} \right)_+.$$

Also, $\ln(2SAT m_T t_k^2) \leq \ln(2SAT^3 m_T)$. Therefore,

$$\begin{aligned}
 (III) &\leq \frac{\gamma m_T}{1-\gamma} \sqrt{2 \ln \frac{1}{1-\underline{\alpha}}} \sum_{k=1}^T I_k^T \sum_{i=1}^{L_k} \frac{\mathbb{I}\{L_k \leq m_T\} \mathbb{I}\{\mathcal{B}_k\}}{\sqrt{N_{t_k}(s_{k,i}, a_{k,i}) + S}} \\
 &+ \frac{\gamma m_T}{1-\gamma} \sqrt{2} \sum_{k=1}^T I_k^T \sum_{i=1}^{L_k} \frac{\mathbb{I}\{L_k \leq m_T\} \mathbb{I}\{\mathcal{B}_k\} \sqrt{\left(\ln \frac{(S+1)(\bar{T}+SA)\sqrt{\bar{T}}}{SA \delta \ln 2 (N_{t_k}(s_{k,i}, a_{k,i})+S)}\right)_+}}{\sqrt{N_{t_k}(s_{k,i}, a_{k,i}) + S}} \\
 &+ \frac{\gamma m_T}{1-\gamma} \sqrt{2 \ln(2SAT^3 m_T)} \sum_{k=1}^T I_k^T \sum_{i=1}^{L_k} \frac{\mathbb{I}\{L_k \leq m_T\} \mathbb{I}\{\mathcal{B}_k\}}{\sqrt{N_{t_k}(s_{k,i}, a_{k,i}) + S}}.
 \end{aligned}$$

The short augmented steps in (III) consist of the first T real interactions plus, only if the last pseudo-episode is short, at most m_T additional proof-only steps. Hence their total number is at most $\bar{T} = T + m_T$. On \mathcal{B}_k , for time within pseudo-episode k ,

$$N_t(s_t, a_t) + S \leq 2(N_{t_k}(s_t, a_t) + S).$$

Thus the two count-sums without logarithmic weights satisfy

$$\sum_{k=1}^T I_k^T \sum_{i=1}^{L_k} \frac{\mathbb{I}\{L_k \leq m_T\} \mathbb{I}\{\mathcal{B}_k\}}{\sqrt{N_{t_k}(s_{k,i}, a_{k,i}) + S}} \leq \sqrt{2} \sum_{t=1}^{\bar{T}} \frac{1}{\sqrt{N_t(s_t, a_t) + S}} \leq \sqrt{8SA\bar{T}}.$$

For the logarithmically weighted sum, using the definition of M_T , the same argument gives

$$\begin{aligned}
 &\sum_{k=1}^T I_k^T \sum_{i=1}^{L_k} \frac{\mathbb{I}\{L_k \leq m_T\} \mathbb{I}\{\mathcal{B}_k\} \sqrt{\left(\ln \frac{(S+1)(\bar{T}+SA)\sqrt{\bar{T}}}{SA \delta \ln 2 (N_{t_k}(s_{k,i}, a_{k,i})+S)}\right)_+}}{\sqrt{N_{t_k}(s_{k,i}, a_{k,i}) + S}} \\
 &\leq \sqrt{8SA(\bar{T} + S^2A)} \left(\ln \left(1 + \frac{SA M_T}{\bar{T} + S^2A} \right) + 2 \right).
 \end{aligned}$$

Combining these bounds yields

$$\begin{aligned}
 \mathbb{E}[(III)] &\leq \frac{\gamma m_T}{1-\gamma} \left(\sqrt{16SA\bar{T} \ln \frac{1}{1-\underline{\alpha}}} + \sqrt{16SA(\bar{T} + S^2A)} \left(\ln \left(1 + \frac{SA M_T}{\bar{T} + S^2A} \right) + 2 \right) \right. \\
 &\quad \left. + \sqrt{16SA\bar{T} \ln(2SAT^3 m_T)} \right).
 \end{aligned}$$

Combining the previous estimates proves (EC.21).

For part (ii), define $\tilde{\Delta}_{k,i} := V_k(s_{k,i}) - V_{\phi_k, \underline{\alpha}}^{\pi_k}(s_{k,i})$. By Lemma 1(ii), $V_{\phi_k, \underline{\alpha}}^*(s) \leq V_k(s)$ for all $s \in \mathcal{S}$, so $V_{\phi_k, \underline{\alpha}}^*(s_{k,i}) - V_{\phi_k, \underline{\alpha}}^{\pi_k}(s_{k,i}) \leq \tilde{\Delta}_{k,i}$. Hence $BR\text{-}R(T) \leq \mathbb{E}[\sum_{k=1}^T I_k^T \sum_{i=1}^{L_k} \tilde{\Delta}_{k,i}]$.

Define \mathcal{P}_k^2 as the event that, for all $(s, a) \in \mathcal{S} \times \mathcal{A}$,

$$\left| (\bar{P}_k(\cdot | s, a) - P_{s,a}^c)^\top V_{\phi_k, \underline{\alpha}}^{\pi_k} \right| \leq \frac{1}{1-\gamma} \sqrt{\frac{2 \ln(2SAT m_T t_k^2)}{N_{t_k}(s, a) + S}}.$$

Then $\mathbb{P}((\mathcal{P}_k^2)^c | \mathcal{F}_{t_k}) \leq 1/(T m_T t_k^2)$, and therefore $\mathbb{P}((\mathcal{P}_k^1 \cap \mathcal{P}_k^2)^c | \mathcal{F}_{t_k}) \leq 2/(T m_T t_k^2)$.

On \mathcal{P}_k^2 , Lemma 9 gives, for each $i \geq 1$,

$$E_{k,i}^- \leq \frac{1}{1-\gamma} \sqrt{\frac{2 \ln \frac{1}{\underline{\alpha}}}{N_{t_k}(s_{k,i}, a_{k,i}) + S}} + \frac{1}{1-\gamma} \sqrt{\frac{2 \ln(2SAT m_T t_k^2)}{N_{t_k}(s_{k,i}, a_{k,i}) + S}}.$$

As in part (i), splitting only according to $\mathcal{P}_k^1 \cap \mathcal{P}_k^2$ and using Lemma 3, the same argument gives

$$\begin{aligned} BR-R(T) &\leq \frac{\gamma m_T}{1-\gamma} \left(\sqrt{16SA\bar{T} \ln \frac{1}{1-\underline{\alpha}}} + \sqrt{16SA(\bar{T} + S^2A) \left(\ln \left(1 + \frac{SA M_T}{\bar{T} + S^2A} \right) + 2 \right)} \right) \\ &\quad + \sqrt{16SA\bar{T} \ln \frac{1}{\underline{\alpha}}} + 2\sqrt{16SA\bar{T} \ln(2SAT^3 m_T)} \\ &\quad + \frac{2\gamma SA}{1-\gamma} m_T^2 \lceil \log_2 m_T \rceil + \frac{\pi^2}{3(1-\gamma)} + 2\mathfrak{I}_T. \end{aligned}$$

This proves (EC.22). \square

Theorem 4 (Restatement of Theorem 2). *For $\delta > 0$, $\underline{\alpha} \in (0, 1)$, and $T \geq S^2A$,*

$$BR(T) \leq \tilde{O} \left(\frac{\gamma \sqrt{SAT \ln \frac{e}{1-\underline{\alpha}}}}{(1-\gamma)^2} + \frac{\delta SA \sqrt{T}}{(1-\gamma)^2} + \frac{SA}{(1-\gamma)^3} \right),$$

and

$$BR-R(T) \leq \tilde{O} \left(\frac{\gamma \sqrt{SAT \ln \frac{1}{\min\{1-\underline{\alpha}, \underline{\alpha}\}}}}{(1-\gamma)^2} + \frac{SA}{(1-\gamma)^3} \right),$$

where $\tilde{O}(\cdot)$ omits polylogarithmic factors in $S, A, T, 1/\delta$, and logarithms of $1/(1-\gamma)$. In particular, if $\delta = \frac{1}{\sqrt{SA}}$ in AQ-BRMDP, then

$$BR(T) \leq \tilde{O} \left(\frac{\gamma \sqrt{SAT \ln \frac{e}{1-\underline{\alpha}}}}{(1-\gamma)^2} + \frac{\sqrt{SAT}}{(1-\gamma)^2} + \frac{SA}{(1-\gamma)^3} \right).$$

Proof. We first prove the bounds for arbitrary $\delta > 0$. By Theorem 3,

$$m_T = \tilde{O} \left(\frac{1}{1-\gamma} \right), \quad m_T^2 \lceil \log_2 m_T \rceil = \tilde{O} \left(\frac{1}{(1-\gamma)^2} \right).$$

Therefore,

$$\frac{\gamma SA}{1-\gamma} m_T^2 \lceil \log_2 m_T \rceil = \tilde{O} \left(\frac{SA}{(1-\gamma)^3} \right).$$

Also $\mathfrak{I}_T = \tilde{O}((1-\gamma)^{-1})$, which is absorbed by $\tilde{O}(SA/(1-\gamma)^3)$.

Since $\bar{T} = T + m_T$, the square-root terms involving \bar{T} are bounded by the corresponding T -terms plus lower-order terms that are absorbed by $\tilde{O}(SA/(1-\gamma)^3)$. Moreover, the logarithmic factor involving M_T contributes only polylogarithmic dependence on $S, A, T, 1/\delta$, and $1/(1-\gamma)$. Since $T \geq S^2A$, the term $\sqrt{SA(\bar{T} + S^2A)}$ is absorbed, up to lower-order terms, by \sqrt{SAT} . For the true-optimal benchmark, this pure \sqrt{SAT} term is absorbed into $\sqrt{SAT \ln \frac{e}{1-\underline{\alpha}}}$ because $\ln \frac{e}{1-\underline{\alpha}} \geq 1$. Substituting these estimates into (EC.21) yields

$$BR(T) \leq \tilde{O} \left(\frac{\gamma \sqrt{SAT \ln \frac{e}{1-\underline{\alpha}}}}{(1-\gamma)^2} + \frac{\delta SA \sqrt{T}}{(1-\gamma)^2} + \frac{SA}{(1-\gamma)^3} \right).$$

For the robust-optimal benchmark, since $\min\{1 - \underline{\alpha}, \underline{\alpha}\} \leq 1/2$, the pure \sqrt{SAT} term is absorbed by $\sqrt{SAT \ln \frac{1}{\min\{1 - \underline{\alpha}, \underline{\alpha}\}}}$. Substituting the same estimates into (EC.22) gives

$$BR-R(T) \leq \tilde{O} \left(\frac{\gamma \sqrt{SAT \ln \frac{1}{\min\{1 - \underline{\alpha}, \underline{\alpha}\}}}}{(1 - \gamma)^2} + \frac{SA}{(1 - \gamma)^3} \right).$$

Finally, if $\delta = 1/\sqrt{SA}$, then

$$\frac{\delta SA \sqrt{T}}{(1 - \gamma)^2} = \frac{\sqrt{SAT}}{(1 - \gamma)^2}.$$

Substituting this into the arbitrary- δ bound for $BR(T)$ gives the stated special case; the $BR-R(T)$ bound does not contain the $\delta SA \sqrt{T}/(1 - \gamma)^2$ term and is therefore unchanged up to hidden polylogarithmic factors. \square

EC.7 Implementation Details

This appendix gives the implementation details for the experiments in Section 5. For the finite-state experiments, the per-transition reward function $r(s, a, s')$ is known and deterministic, while the entire transition kernel is treated as unknown. When the reward depends on the next state, as in FrozenLake, expected one-step rewards are computed under the sampled posterior transition model. The agent maintains an independent Dirichlet posterior over each transition vector $P_{s,a}^c$ and updates the posterior parameters using the observed transition counts. For the continuous-state FrozenLake experiment, the transition kernel is parameterized by some stochastic components; details are given in Appendix EC.7.7.

EC.7.1 Value Iteration for the Approximate α_k -quantile BR-MDP

At the beginning of pseudo-episode k , AQ-BRMDP first updates the posterior parameters ϕ_k using the history data and then computes the adaptive quantile schedule α_k . These two quantities define the α_k -quantile BR-MDP to be solved in the current pseudo-episode. The exact posterior quantiles in Bellman backups are generally not available in closed form. We therefore replace the exact posterior quantile by an empirical quantile computed from posterior samples, leading to the approximate α_k -quantile BR-MDP used in implementation. For a value vector V , state-action pair (s, a) , and quantile level $\alpha_k(s, a)$, we draw posterior transition samples $P_{s,a}^1, \dots, P_{s,a}^M \stackrel{\text{i.i.d.}}{\sim} \text{Dir}(\phi_k(s, a))$ and compute the sampled one-step Bellman targets $Z_j = \sum_{s' \in \mathcal{S}} P_{s,a}^j(s') [r(s, a, s') + \gamma V(s')]$. We then sort $Z_{(1)} \leq \dots \leq Z_{(M)}$ and use $Z_{(\lceil M \alpha_k(s, a) \rceil)}$ as the empirical posterior quantile.

Monte Carlo budget for quantile estimation. The posterior-sampling budget used in each Bellman backup controls the Monte Carlo error of the empirical quantile estimator. To choose this budget across different quantile levels, we use the classical asymptotic normal approximation for sample quantiles. If \hat{q}_α is the empirical α -quantile computed from m independent samples of a scalar random variable with density g positive at its α -quantile q_α , then the leading variance term is proportional to

$$\frac{\alpha(1 - \alpha)}{m g(q_\alpha)^2}.$$

Since the exact density of the sampled Bellman target depends on both the posterior parameter and the current value vector, we use the standard normal distribution as a reference distribution to choose how the sample size varies across quantile levels. This choice allocates more posterior samples to tail quantiles.

For AQ-BRMDP, at pseudo-episode k and state-action pair (s, a) , let $q_{k,s,a} := \Phi^{-1}(\alpha_k(s, a))$, and let φ_{std} denote the standard normal density. The number of posterior samples used to estimate the quantile from (s, a) is chosen as

$$n_{k,s,a} = \min \left\{ 2048, \left\lceil c_{n_{\text{samples}}} \frac{\alpha_k(s, a)(1 - \alpha_k(s, a))}{\varphi_{\text{std}}(q_{k,s,a})^2} \right\rceil \right\}. \quad (\text{EC.23})$$

For the fixed-level baselines BR-MDP- α with $\alpha \in \{0.1, 0.3, 0.5\}$, we use the same rule with $\alpha_k(s, a)$ replaced by the corresponding fixed value α .

Algorithm EC.2 Value Iteration for the Approximate α_k -quantile BR-MDP

- 1: **Input:** Posterior parameters ϕ_k , approximate optimal value in pseudo-episode $k - 1$ \widehat{V}_{k-1} , quantile schedule α_k , per-transition reward function r , discount factor γ , Monte Carlo budget coefficient $c_{n_{\text{samples}}}$, tolerance ε_{VI} , maximum number of iterations M_{VI}
 - 2: **for all** $(s, a) \in \mathcal{S} \times \mathcal{A}$ **do**
 - 3: Compute $n_{k,s,a}$ from (EC.23) and set $\ell_{k,s,a} \leftarrow \lceil n_{k,s,a} \alpha_k(s, a) \rceil$
 - 4: Draw and fix posterior samples $P_{s,a}^1, \dots, P_{s,a}^{n_{k,s,a}} \stackrel{\text{i.i.d.}}{\sim} \text{Dir}(\phi_k(s, a))$
 - 5: **end for**
 - 6: Initialize $V^{(0)} \leftarrow \widehat{V}_{k-1}$
 - 7: **for** $m = 0, 1, \dots, M_{\text{VI}} - 1$ **do**
 - 8: **for all** $(s, a) \in \mathcal{S} \times \mathcal{A}$ **do**
 - 9: Using the fixed posterior samples, compute

$$Z_j^{(m)}(s, a) \leftarrow \sum_{s' \in \mathcal{S}} P_{s,a}^j(s') [r(s, a, s') + \gamma V^{(m)}(s')], \quad j = 1, \dots, n_{k,s,a}.$$
 - 10: Sort $Z_{(1)}^{(m)}(s, a) \leq \dots \leq Z_{(n_{k,s,a})}^{(m)}(s, a)$
 - 11: Set $Q_k^{(m+1)}(s, a) \leftarrow Z_{(\ell_{k,s,a})}^{(m)}(s, a)$
 - 12: **end for**
 - 13: Set $V^{(m+1)}(s) \leftarrow \max_{a \in \mathcal{A}} Q_k^{(m+1)}(s, a)$ for all $s \in \mathcal{S}$
 - 14: **if** $\|V^{(m+1)} - V^{(m)}\|_{\infty} \leq \varepsilon_{\text{VI}}$ **then**
 - 15: **break**
 - 16: **end if**
 - 17: **end for**
 - 18: Set $\widehat{V}_k \leftarrow V^{(m+1)}$
 - 19: For each $s \in \mathcal{S}$, choose $\widehat{\pi}_k(s) \in \arg \max_{a \in \mathcal{A}} Q_k^{(m+1)}(s, a)$
 - 20: **return** \widehat{V}_k and $\widehat{\pi}_k$
-

The posterior transition samples in Algorithm EC.2 are drawn once at the beginning of pseudo-episode k and held fixed throughout the value-iteration loop. Hence the empirical-quantile Bellman operator is deterministic within the pseudo-episode, and the stopping criterion is applied to a fixed sample-average approximation of the α_k -quantile BR-MDP. The fixed-level baselines BRMDP-0.1, BRMDP-0.3, and BRMDP-0.5 use Algorithm EC.2 with $\alpha_k(s, a) \equiv 0.1, 0.3$, and 0.5 , respectively.

EC.7.2 Implementations of Continuing PSRL

Continuing PSRL uses the same pseudo-episode mechanism as AQ-BRMDP. At the beginning of pseudo-episode k , it samples one transition kernel \widetilde{P}_k from the current posterior by drawing $\widetilde{P}_{k,s,a} \sim \text{Dir}(\phi_k(s, a))$ independently for all (s, a) . It then solves the sampled discounted MDP using standard value iteration and executes a greedy policy $\widetilde{\pi}_k$ throughout pseudo-episode k . When rewards are transition-dependent, the one-step reward in the sampled MDP is evaluated as $\sum_{s'} \widetilde{P}_{k,s,a}(s') r(s, a, s')$, so Continuing PSRL also avoids using the true expected reward under P^c during learning.

EC.7.3 Finite-State Experiment Schematics

Figure EC.3 provides schematic diagrams for the two finite-state experiment families used in Section 5.

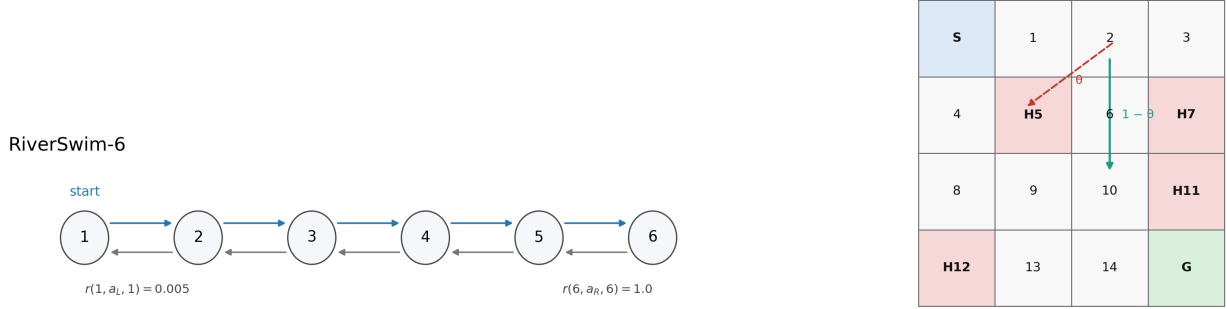


Figure EC.3: Finite-state experiment schematics: RiverSwim-6 (left) and risky-branch FrozenLake (right). In the FrozenLake schematic, the shortcut at (2, Down) moves the agent to state 10 with probability $1 - \theta$ and to the sticky hole at state 5 with probability θ .

EC.7.4 Experiment-Specific Settings and Evaluation Details

For AQ-BRMDP, the floor parameter in the adaptive schedule is set to $\underline{\alpha} = 0.2$ in all finite-state experiments unless otherwise stated. In all tabular BR-MDP planning calls, we use value-iteration tolerance $\varepsilon_{VI} = 10^{-8}$ and maximum iteration count $M_{VI} = 10,000$. The same stopping rule and iteration cap are used for Continuing PSRL, fixed-quantile BR-MDP, and AQ-BRMDP planning. The finite-state RiverSwim and risky-branch FrozenLake experiments were run on a MacBook using CPU execution without GPU acceleration. These experiments were substantially less computationally demanding than the continuous-state FrozenLake experiment reported below.

RiverSwim. The discount factor is $\gamma = 0.9$, and the total interaction horizon is $T = 4500$. We set the constant in (EC.23) and (14) to $(c_{n_{\text{samples}}}, \delta) = (150, 5)$ and $(200, 10)$ respectively for RiverSwim-6 and RiverSwim-10. The plots for RiverSwim-6 and RiverSwim-10 are truncated to the first 2000 and 4000 time steps, respectively. The same truncation windows are used for the corresponding occupancy heatmaps.

Risky-branch FrozenLake. In risky-branch FrozenLake experiments, the discount factor $\gamma = 0.8$, and total interaction horizon $T = 4500$. We set the constant in (EC.23) and (14) to $(c_{n_{\text{samples}}}, \delta) = (250, 10)$.

EC.7.5 Estimation of the Posterior α -Quantile Value

We estimate the posterior α -quantile value by evaluating the current policy under posterior samples of the transition kernel. For each independent run, each algorithm, and diagnostic time t , we take the current posterior parameter ϕ_t and the current policy π_t . We then draw $M = 147$ independent transition kernels by drawing $P_{s,a}^{(m)} \sim \text{Dir}(\phi_t(s, a))$, $m = 1, \dots, M$, independently for all (s, a) . For each sampled transition kernel $P^{(m)}$, we compute the value of π_t by exact policy evaluation. In particular, letting $P^{(m), \pi_t}(s, s') := P_{s, \pi_t(s)}^{(m)}(s')$ and $r^{(m), \pi_t}(s) := \sum_{s' \in \mathcal{S}} P_{s, \pi_t(s)}^{(m)}(s') r(s, \pi_t(s), s')$, we compute $V_{P^{(m)}}^{\pi_t} = (I - \gamma P^{(m), \pi_t})^{-1} r^{(m), \pi_t}$. We then form the M sampled values at the initial state, $Y_m := V_{P^{(m)}}^{\pi_t}(s_0)$ for $m = 1, \dots, M$, and let $Y_{(1)} \leq \dots \leq Y_{(M)}$ denote their order statistics. The empirical estimate of the posterior 0.1-quantile value is

$$\widehat{V}_{\phi_t, 0.1}^{\pi_t, \text{q}}(s_0) := Y_{(\lceil 0.1M \rceil)}. \quad (\text{EC.24})$$

We set $M = 147$ according to (EC.23) with $c_{n_{\text{samples}}} = 50$. This metric is computed every 200 time steps. For each diagnostic time, we average the estimates over 100 independent runs, and the 95% confidence bands are computed across these independent runs.

EC.7.6 Sensitivity Analysis for the Schedule Parameter

We examine sensitivity to the schedule parameter δ on standard FrozenLake without the risky branch, holding the remaining settings fixed as described in Section 5.2. We compare $\delta \in \{5, 10, 15\}$ over 100 independent runs per setting. These small differences in Figure EC.4 and Table EC.1 suggest that AQ-BRMDP is not materially sensitive to δ over the range tested.

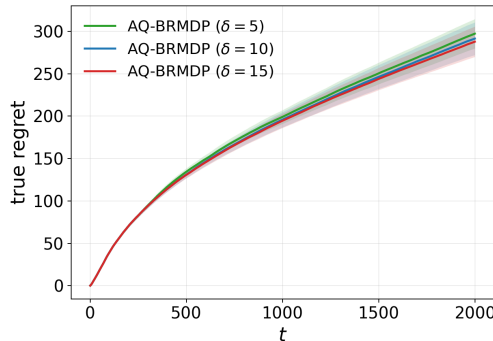


Figure EC.4: Sensitivity of AQ-BRMDP to the schedule parameter δ on FrozenLake without the risky branch. The plot shows cumulative true regret.

Table EC.1: Final cumulative true regret in the sensitivity study. Each entry reports the mean over 100 runs. Percentages are reductions relative to the $\delta = 5$ setting.

δ	Final cumulative regret	Reduction
5	297.2396	0.00%
10	291.4018	1.96%
15	287.7603	3.19%

EC.7.7 Continuous-State FrozenLake Experiment

We further evaluate AQ-BRMDP in a continuous-state version of FrozenLake. In this experiment, the state space is continuous, the posterior is placed on a parametric transition model, and the resulting Bellman backups are approximated using neural fitted Q iteration.

Environment. The state space is $[0, 4]^2$, partitioned into the same 4×4 cells as the discrete FrozenLake layout. The start state is $(0.5, 0.5)$, the hole cells are $\{5, 7, 11, 12\}$, and the goal cell is 15. The action space remains $\{\text{Left, Right, Up, Down}\}$. A transition receives reward 1 if the next state enters the goal cell and reward 0 otherwise. From the goal cell, the next state is sampled from the known uniform reset distribution over the non-hole, non-goal cells.

For ordinary cells, the realized movement direction is the intended direction with probability 0.50 and one of the two perpendicular directions with probability 0.25 each. For hole cells, the agent moves in the intended direction with probability $p_h = 0.20$ and otherwise remains in place. The continuous movement length is $L = \ell_0 + U$, where $\ell_0 = 0.75$ and $U \sim \text{Unif}(0, \theta_L)$ with true value $\theta_L = 0.50$. If a candidate next state leaves $[0, 4]^2$, the agent remains in the current state.

Posterior model. The unknown transition parameters are $(p_{\text{slip}}, p_h, \theta_L)$. We use the conjugate priors $p_{\text{slip}} \sim \text{Dir}(1, 1, 1)$, $p_h \sim \text{Beta}(1, 1)$, and $\theta_L \sim \text{Pareto}(a_0, x_0)$ with $a_0 = 2$ and $x_0 = 0.25$. The simulator records latent primitives: M_t for the ordinary-cell movement mode, E_t for the hole mobility indicator, and L_t for the attempted movement length when a movement is activated. The Dirichlet posterior is updated from counts of M_t , the Beta posterior is updated from counts of E_t , and the Pareto posterior is updated from observations of $U_t = L_t - \ell_0$. Goal reset transitions do not update the posterior.

Neural fitted Q approximation. The Q-function is represented by a neural network $Q_\omega(s, a)$ with architecture $20 \rightarrow 64 \rightarrow 64 \rightarrow 4$, where the four outputs correspond to the four actions. The 20 input features consist of the normalized two-dimensional coordinates, a 16-dimensional cell one-hot vector, and two hole/goal indicators. At the start of each pseudo-episode, the network is warm-started from the previous pseudo-episode; it is not reinitialized.

For a sampled posterior model θ^b and a Q-function Q , define the posterior-model Bellman target $G^b(s, a; Q) := \mathbb{E}_{s' \sim P_{\theta^b}(\cdot | s, a)} [R(s, a, s') + \gamma \max_{a'} Q(s', a')]$.

For AQ-BRMDP, the Bellman target is the empirical $\alpha_k(s, a)$ -quantile of $G^b(s, a; Q)$ over posterior samples. For PSRL, a single posterior model is sampled and the risk-neutral Bellman target under that sampled model is used. The expectations in these targets are estimated by Monte Carlo simulation from the corresponding model.

Adaptive quantile schedule in the continuous setting. The normalization set consists of the 15 cell centers excluding the goal center $(3.5, 3.5)$. For each queried (s, a) , the posterior predictive uncertainty $u_k(s, a)$ is computed as the standard deviation of $G^b(s, a; Q_{\omega_{k-1}})$ across posterior samples, and $c_k(s, a) = 1/(u_k(s, a) + \varepsilon)$. Let \bar{c}_k be the average of $c_k(\tilde{s}, a)$ over the non-goal center states and actions. For non-goal states, $\alpha_k(s, a) = \text{clip}\left(1 - \delta \frac{c_k(s, a)}{\bar{c}_k} g_k, \underline{\alpha}, 0.95\right)$, and $g_k = \frac{\log(2k)}{\sqrt{k}}$.

For goal states, all actions are equivalent and we set $\alpha_k(s, a) = \text{clip}(1 - \delta g_k, \underline{\alpha}, 0.95)$. The posterior sample budget used to estimate each quantile is selected by the same rule as in (EC.23) and capped at 800 posterior samples.

Algorithm EC.3 Continuous-State AQ-BRMDP with Neural Fitted Q Approximation

- 1: **Input:** initial posterior, initial Q-network parameter ω_0 , schedule parameters, and replay buffer $\mathcal{B} \leftarrow \emptyset$
 - 2: Initialize pseudo-episode index $k \leftarrow 0$ and restart indicator $X_1 \leftarrow 0$
 - 3: **for** $t = 1, \dots, T$ **do**
 - 4: **if** $X_t = 0$ **then**
 - 5: $k \leftarrow k + 1$
 - 6: Update the posterior using the observed latent primitives
 - 7: Draw posterior model samples $\{\theta_k^b\}$ from the current posterior
 - 8: Compute \bar{c}_k over non-goal center states and fix the rule defining $\alpha_k(s, a)$ for this pseudo-episode
 - 9: $\omega_k \leftarrow \text{FitQ}(\omega_{k-1}, \alpha_k, \{\theta_k^b\}, \mathcal{B})$ using fitted-Q regression
 - 10: **end if**
 - 11: Take action $a_t \in \arg \max_{a \in \mathcal{A}} Q_{\omega_k}(s_t, a)$
 - 12: Observe s_{t+1} , reward r_t , and latent primitives when applicable
 - 13: Append the transition and latent primitives to \mathcal{B}
 - 14: Sample $X_{t+1} \sim \text{Bernoulli}(\gamma)$ if $t < T$
 - 15: **end for**
-

The fitted-Q subroutine initializes at ω_{k-1} and repeats a standard fitted-Q loop: sample training states, construct clipped Monte Carlo Bellman targets for each state-action pair, and regress Q_ω onto those targets. For AQ-BRMDP, the target is the empirical $\alpha_k(s, a)$ -quantile over posterior models; for PSRL, it is the risk-neutral target under one sampled model.

The continuous-state experiment compares AQ-BRMDP with a continuous-state PSRL baseline using the same pseudo-episode mechanism, posterior model, Q-network architecture, and fitted-Q solver.

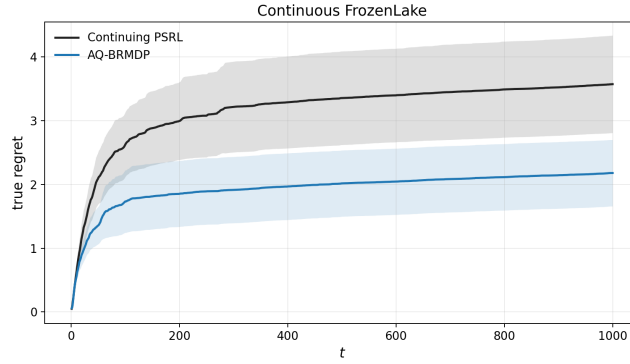


Figure EC.5: Cumulative true regret in continuous-state FrozenLake.

The continuous-state results show that AQ-BRMDP can be implemented with a parametric posterior model and neural fitted-Q approximation in a continuous-state space. Figure EC.5 shows that AQ-BRMDP outperforms the continuous-state PSRL baseline with smaller cumulative true regret while retaining the adaptive quantile mechanism used in the finite-state experiments.

The continuous-state FrozenLake experiments were run on a single NVIDIA GeForce RTX 4090 GPU with 24 GB GPU memory. The mean runtime per independent run was 21.2 minutes for AQ-BRMDP and 5.5 minutes for Continuing PSRL, with the difference mainly due to posterior quantile estimation.